8 Interference mitigation and awareness for improved reliability

Huseyin Arslan, Serhan Yarkan, Mustafa E. Sahin, and Sinan Gezici

Wireless systems are commonly affected by interference from various sources. For example, a number of users that operate in the same wireless network can result in multiple-access interference (MAI). In addition, for ultrawideband (UWB) systems, which operate at very low power spectral densities, strong narrowband interference (NBI) can have significant effects on the communications reliability. Therefore, interference mitigation and awareness are crucial in order to realize reliable communications systems. In this chapter, pulse-based UWB systems are considered, and the mitigation of MAI is investigated first. Then, NBI avoidance and cancelation are studied for UWB systems. Finally, interference awareness is discussed for short-rate communications, next-generation wireless networks, and cognitive radios.

8.1 Mitigation of multiple-access interference (MAI)

In an impulse radio ultrawideband (IR-UWB) communications system, pulses with very short durations, commonly less than one nanosecond, are transmitted with a low-duty cycle, and information is carried by the positions or the polarities of pulses [1–5]. Each pulse resides in an interval called "frame", and the positions of pulses within frames are determined according to time-hopping (TH) sequences specific to each user. The low-duty cycle structure together with TH sequences provide a multiple-access capability for IR-UWB systems [6].

Although IR-UWB systems can theoretically accommodate a large number of users in a multiple-access environment [2, 4], advanced signal processing techniques are necessary in practice in order to mitigate the effects of interfering users on the detection of information symbols efficiently [6]. In this section, various MAI mitigating receiver structures are studied first. Then, the effects of coding design on the mitigation of MAI are investigated.

8.1.1 Receiver design for MAI mitigation

In this section, optimal and suboptimal detector structures with various levels of computational complexity are investigated in order to mitigate the effects of MAI [6]. A synchronous IR-UWB system with K users is considered, and the transmitted signal

from user k is expressed as

$$s_{\text{tx}}^{(k)}(t) = \sqrt{\frac{E_k}{N_f}} \sum_{j=-\infty}^{\infty} d_j^{(k)} \, b_{\lfloor j/N_f \rfloor}^{(k)} \, p_{\text{tx}}\left(t - jT_f - c_j^{(k)} T_c - a_{\lfloor j/N_f \rfloor}^{(k)} \delta\right) , \tag{8.1}$$

where $p_{\text{tx}}(t)$ is the transmitted UWB pulse, E_k is the symbol energy of user k, T_f is the "frame" time, and N_f is the number of pulses representing one information symbol [7]. For pulse amplitude modulation (PAM), $a_{\lfloor j/N_f \rfloor}^{(k)} = 0$, $\forall j, k$, and the information symbol $b_{\lfloor j/N_f \rfloor}^{(k)}$ determines the pulse amplitude. On the other hand, for M-ary pulse position modulation (PPM), $b_{\lfloor j/N_f \rfloor}^{(k)} = 1$, $\forall j, k$, and the information is carried by $a_{\lfloor j/N_f \rfloor}^{(k)} \in \{0, 1, \ldots, M-1\}$ with δ denoting the modulation index [4, 6, 8]. In this section, PAM is considered, and the readers are referred to references [6, 9] for extensions to PPM.

In (8.1), $c_j^{(k)} \in \{0, 1, \ldots, N_c - 1\}$ denotes the TH sequence for user k, where N_c denotes the number of chips in a frame; i.e., $N_c = T_f / T_c$. TH sequences allow the channel to be shared by multiple users without causing catastrophic collisions between the pulses from different users. In order to further reduce the effects of MAI, the polarity codes, $d_j^{(k)} \in \{-1, 1\}$, can be employed, which also help reduce the spectral lines in the power spectral density (PSD) of the transmitted signal [10–12]. In the following, it is assumed that the receiver for user k knows its TH and polarity codes.

The IR-UWB signal in (8.1) can also be expressed as a code division multiple access (CDMA) signal by introducing the following sequence [9, 11]:

$$s_j^{(k)} = \begin{cases} d_{\lfloor j/N_c \rfloor}^{(k)}, & \text{if } j - N_c \lfloor j/N_c \rfloor = c_{\lfloor j/N_c \rfloor}^{(k)} \\ 0, & \text{otherwise} \end{cases} . \tag{8.2}$$

Then, (8.1) becomes

$$s_{\text{tx}}^{(k)}(t) = \sqrt{\frac{E_k}{N_f}} \sum_{j=-\infty}^{\infty} s_j^{(k)} \, b_{\lfloor j/(N_f N_c) \rfloor}^{(k)} \, p_{\text{tx}}(t - jT_c) , \tag{8.3}$$

which is in the form of a CDMA signal with $s_j^{(k)}$ defining a generalized spreading sequence that can take values from the set $\{-1, 0, +1\}$ [6, 9, 11, 13]. Therefore, multiple-access mitigation techniques or multiuser detection (MUD) algorithms developed for CDMA systems can be adopted for IR-UWB systems as well [8, 13–16]. However, the complexity of those techniques is often quite high, and the signaling structure of IR-UWB systems allows for simpler multiple-access mitigation algorithms which are specifically designed to exploit that structure [6, 14], and which are the main focus of this section.

Assuming a tapped-delay-line channel model with multipath resolution T_c, the discrete channel $\boldsymbol{\alpha}^{(k)} = [\alpha_1^{(k)} \cdots \alpha_L^{(k)}]$ is adopted for user k [7]. Then, the received signal can be stated as

$$\begin{aligned} r(t) = \sum_{k=1}^{K} \sqrt{\frac{E_k}{N_f}} \sum_{j=-\infty}^{\infty} \sum_{l=1}^{L} \alpha_l^{(k)} d_j^{(k)} \, b_{\lfloor j/N_f \rfloor}^{(k)} \\ \times p_{\text{rx}}\left(t - jT_f - c_j^{(k)} T_c - (l-1)T_c\right) + \sigma_n n(t) , \end{aligned} \tag{8.4}$$

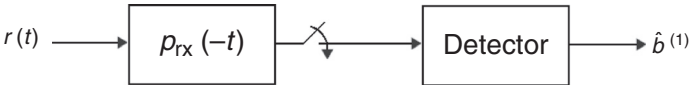

Figure 8.1 A receiver structure with chip-rate sampling.

where $p_{\text{rx}}(t)$ is the received unit-energy UWB pulse, which is usually modeled as the derivative of $p_{\text{tx}}(t)$ due to the effects of the antenna, and $n(t)$ is zero-mean additive white Gaussian noise (AWGN) with unit spectral density.

After filtering and amplification, the front-end of the receiver can perform different operations on the received analog signal with varying levels of complexity and accuracy. In that respect, the receivers can be classified as [17]:

- direct sampling receivers;
- matched filter receivers;
- energy detection receivers.

Although direct sampling can facilitate perfect reconstruction of the received signal from its samples, it requires very high sampling rates on the order of a few GHz for UWB systems, which results in increased power consumption and complexity for the receiver [18]. On the other hand, energy detection receivers provide a design alternative with low power consumption and complexity [19–22]. However, those benefits are accompanied by performance loss, which can be critical in multiple-access environments.

A matched filter receiver provides a tradeoff between the direct sampling and energy detection approaches in the sense that it can both achieve better performance than energy detection receivers and facilitate designs with lower power consumption and complexity than direct sampling receivers. In addition, depending on the design of the matched filter, various sampling rate options can be obtained. For example, the receiver analog signal can be applied to a filter that is matched to the received pulse shape and the filter output can be sampled at the chip-rate, as shown in Figure 8.1. Since chip-rate sampling can require high-speed analog-to-digital conversion on the order of a few Gbps, a low-cost and low-power alternative is to employ frame-rate sampling via multiple matched filter (equivalently, correlator) branches as shown in Figure 8.2. In that case, each branch collects signals from one of the multipaths. More specifically, considering user 1 as the user of interest, the template signal matches the UWB pulse $p_{\text{rx}}(t)$ and the TH and polarity codes of user 1, and samples are taken at instants when the paths $l \in \mathcal{L}$ arrive in each frame, where $\mathcal{L} = \{l_1, \ldots, l_M\}$ with $M \leq L$. Namely, $s^{(1)}_{\text{temp},l}(t) = d^{(1)}_j p_{\text{rx}}\left(t - c^{(1)}_j T_c - (l-1)T_c\right)$ for $l \in \mathcal{L}$, and the samples are taken at $t = (iN_f)T_f, \ldots, ((i+1)N_f - 1)T_f$ for the ith symbol. In other words, M correlators are used to collect frame-rate samples from M of the L multipath components. Since there can be collisions among various multipath components due to inter-frame interference (IFI), the actual number N of distinct samples per information symbol can be smaller than $N_f M$.

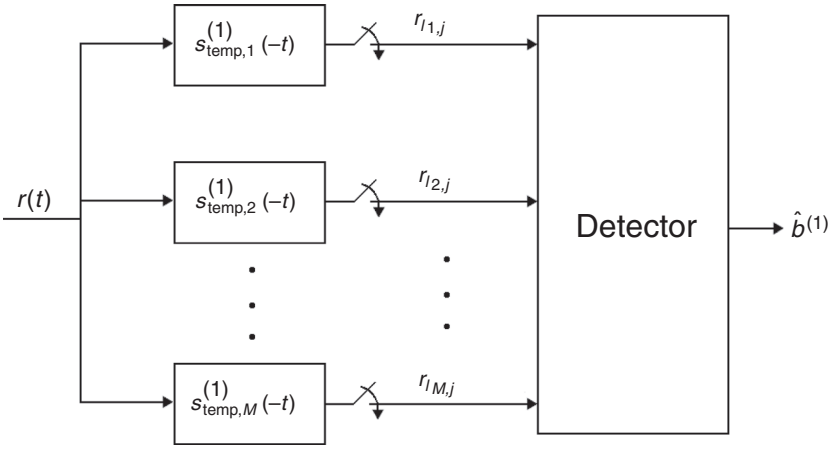

Figure 8.2 A receiver structure with M branches, where frame-rate sampling is employed at each branch.

Based on the receiver front-end in Figure 8.2, the discrete signal at the lth path of the jth frame can be expressed, for the ith information bit, as [7]

$$r_{l,j} = \mathbf{s}_{l,j}^T \mathbf{A} \mathbf{b}_i + n_{l,j} \,, \tag{8.5}$$

for $l = l_1, \ldots, l_M$ and $j = iN_f, \ldots, (i+1)N_f - 1$, where $\mathbf{b}_i = [b_i^{(1)} \cdots b_i^{(K)}]^T$, $n_{l,j} \sim \mathcal{N}(0\,,\, \sigma_n^2)$, and

$$\mathbf{A} = \begin{bmatrix} \sqrt{\frac{E_1}{N_f}} & 0 & \cdots & 0 \\ 0 & \ddots & \ddots & \vdots \\ \vdots & \ddots & \ddots & 0 \\ 0 & \cdots & 0 & \sqrt{\frac{E_K}{N_f}} \end{bmatrix} . \tag{8.6}$$

In addition, $\mathbf{s}_{l,j}$ is a $K \times 1$ vector that is equal to the sum of the desired signal part (SP), IFI, and MAI terms:

$$\mathbf{s}_{l,j} = \mathbf{s}_{l,j}^{(\text{SP})} + \mathbf{s}_{l,j}^{(\text{IFI})} + \mathbf{s}_{l,j}^{(\text{MAI})} \,, \tag{8.7}$$

where the kth elements can be expressed as

$$\left[\mathbf{s}_{l,j}^{(\text{SP})}\right]_k = \begin{cases} \alpha_l^{(1)}\,, & k = 1 \\ 0\,, & k = 2, \ldots, K \end{cases} , \tag{8.8}$$

$$\left[\mathbf{s}_{l,j}^{(\text{IFI})}\right]_k = \begin{cases} d_j^{(1)} \sum_{(n,m)\in\mathcal{A}_{l,j}} d_m^{(1)} \alpha_n^{(1)}\,, & k = 1 \\ 0\,, & k = 2, \ldots, K \end{cases} , \tag{8.9}$$

$$\left[\mathbf{s}_{l,j}^{(\text{MAI})}\right]_k = \begin{cases} 0\,, & k = 1 \\ d_j^{(1)} \sum_{(n,m)\in\mathcal{B}_{l,j}^{(k)}} d_m^{(k)} \alpha_n^{(k)}\,, & k = 2, \ldots, K \end{cases} , \tag{8.10}$$

with

$$\mathcal{A}_{l,j} = \{(n,m) : n \in \{1,\ldots,L\},\ m \in \mathcal{F}_i,\ m \neq j,\\ mT_f + c_m^{(1)}T_c + nT_c = jT_f + c_j^{(1)}T_c + lT_c\} \tag{8.11}$$

and

$$\mathcal{B}_{l,j}^{(k)} = \{(n,m) : n \in \{1,\ldots,L\},\ m \in \mathcal{F}_i,\\ mT_f + c_m^{(k)}T_c + nT_c = jT_f + c_j^{(1)}T_c + lT_c\}\,, \tag{8.12}$$

where $\mathcal{F}_i = \{iN_f,\ldots,(i+1)N_f - 1\}$ [7].

It is observed from (8.11) that $\mathcal{A}_{l,j}$ represents the set of frame and multipath indices of pulses from user 1 that originate from a frame different from the jth one and collide with the lth path of the jth pulse of user 1. Similarly, $\mathcal{B}_{l,j}^{(k)}$ denotes the set of frame and path indices of pulses from user k that collide with the lth path of the jth pulse of user 1 [7].

In the following, it is assumed that there exists a guard interval between adjacent symbols that is equal to the length of the channel impulse response (CIR) so that no inter-symbol interference (ISI) occurs. Therefore, for bit i, only the interference from the pulses in the frames of the current symbol i; namely, from the pulses in frames $iN_f,\ldots,(i+1)N_f - 1$, are taken into account [7]. In addition, a binary modulation with $b_i^{(k)} \in \{-1, 1\}$ is considered in the remainder of the section.

In order to provide intuitive explanations for some of the multiple-access mitigation algorithms below, the special case of the signal model in (8.5) for single-path channels can be useful. In that case, $\alpha_1^{(k)} = 1$ and $\alpha_l^{(k)} = 0$ for $l > 1$ and $\forall k$ are considered. Therefore, one sample is collected from each frame, resulting in the following received signal vector for the 0th symbol of user 1 [6]:

$$\mathbf{r} = [r_{1,0}\ r_{1,1}\ \cdots\ r_{1,N_f-1}]^T, \tag{8.13}$$

where $r_{1,j}$ is as given in (8.5), with the kth element of $\mathbf{s}_{1,j}$ being expressed as

$$\left[\mathbf{s}_{1,j}\right]_k = \begin{cases} 1\,, & k = 1 \\ d_j^{(1)} d_j^{(k)} \mathrm{I}_{\{c_j^{(k)} = c_j^{(1)}\}}\,, & k = 2,\ldots,K \end{cases}. \tag{8.14}$$

Here, $\mathrm{I}_{\{c_j^{(k)} = c_j^{(1)}\}}$ denotes an indicator function that is equal to one if $c_j^{(k)} = c_j^{(1)}$, and zero otherwise. It is noted from (8.14) that, for single-path channels, no IFI exists, and the main source of interference becomes the MAI. The received signal in (8.13) can be expressed in the vector form as

$$\mathbf{r} = \mathbf{SAb} + \mathbf{n}\,, \tag{8.15}$$

where $\mathbf{b} = \left[b_0^{(1)} \cdots b_0^{(K)}\right]^T$, $\mathbf{n}$ is a $K \times 1$ vector of independent and identically distributed (i.i.d.) Gaussian noise components, $\mathbf{n} \sim \mathcal{N}(\mathbf{0}\,,\ \sigma_n^2\mathbf{I})$, and $\mathbf{S}$ is the $N_f \times K$ signature matrix, the jth row of which is given by $\mathbf{s}_{1,j}^T$ in (8.14) [6].

Since IR-UWB systems transmit pulses with a low duty cycle, signals from some of the users may not collide with the pulses of the desired user. In that case, the signals of such users can be excluded from the signal model in (8.15), and a simpler model can be obtained. If K_1 is the number of users colliding with the pulses of user 1, the received signal vector can be expressed as [14]

$$\mathbf{r} = \mathbf{S}_1 \mathbf{A}_1 \mathbf{b}_1 + \mathbf{n} \,, \tag{8.16}$$

where $\mathbf{b}_1$ is a $(K_1 + 1) \times 1$ vector consisting of the information symbols from the first user and the users colliding with that user, $\mathbf{A}_1$ is a diagonal matrix with the first element being the amplitude of the signal from user 1 and the remaining elements being the amplitudes of the users' signals colliding with user 1, and the $N_f \times (K_1 + 1)$ signature matrix $\mathbf{S}_1$ is obtained from $\mathbf{S}$ in (8.15) by removing the columns corresponding to elements that do not collide with the first user [6].

8.1.1.1 Maximum likelihood based detectors

The optimal detector that minimizes the average probability of error is specified by the maximum likelihood (ML) detector for equally likely information symbols [23]. Specifically, the ML detector selects the information symbols that maximize the log-likelihood function. The complexity of the ML detector grows exponentially with the number of users K; namely, $\mathcal{O}(2^K)$ [6, 15, 24]. In order to provide an alternative detector with lower complexity, one can consider the samples at instants only when the pulses from the desired user, user 1, arrives. Then, the following *quasi-ML* detector can be obtained [14]:

$$\hat{b}^{(1)} = \arg \max_{b^{(1)} \in \{-1,1\}} \sum_{\tilde{\mathbf{b}} \in \{-1,1\}^{K_1}} \left\| \mathbf{r} - \mathbf{S}_1 \mathbf{A}_1 \left[b^{(1)} \; \tilde{\mathbf{b}} \right]^T \right\|^2 \,, \tag{8.17}$$

where $\mathbf{r}$, $\mathbf{S}_1$, and $\mathbf{A}_1$ are as in (8.16), and K_1 denotes the number of users colliding with the first user.

It is noted from (8.17) that the complexity of the quasi-ML detector is $\mathcal{O}(2^{K_1})$, which can be significantly lower than that of the optimal ML detector when the number of users colliding with the first user is small. In addition, the quasi-ML detector can be considered as the optimal detector given the received samples only at the instants when the pulses from user 1 arrive. However, compared to the ML detector with chip-rate sampling, the quasi-ML detector suffers from a performance loss [6].

8.1.1.2 Linear detectors

Due to the high computational complexity of ML-based detectors, linear detectors can be preferred in some applications in order to provide low-complexity solutions with reasonable performance [6, 25]. A linear detector obtains a linear combination of the received signal samples, and estimates the information bit as the sign of the combined samples. Namely,

$$\hat{b}^{(1)} = \text{sign} \left\{ \boldsymbol{\theta}^T \mathbf{r} \right\} \,, \tag{8.18}$$

where $\boldsymbol{\theta}$ represents a weighting vector, and $\mathbf{r}$ is the vector of received signal samples. The performance and complexity of linear receivers depend on the approach for setting the weighting vector $\boldsymbol{\theta}$, as discussed below.

Pulse discarding detectors

A simple approach to determine the weighting vector in (8.18) is to discard all the received signal samples that are (significantly) affected by MAI. For example, a blinking receiver (BR) ignores all the samples that are corrupted by any of the pulses of interfering users and makes use of only the uncorrupted pulses [14]. Specifically, based on the received signal model in (8.13), the weighting vector in (8.18) is expressed for a BR as

$$[\boldsymbol{\theta}]_j = \begin{cases} 1\,, & \text{if } [\mathbf{s}_{1,j}]_2 = \cdots = [\mathbf{s}_{1,j}]_K = 0 \\ 0\,, & \text{otherwise} \end{cases} \tag{8.19}$$

for $j = 1, \ldots, N_f$, where $[\boldsymbol{\theta}]_j$ denotes the jth component of $\boldsymbol{\theta}$.

It should be noted that a BR needs to know which samples are affected by interference in order to determine the weighting vector in (8.19). In addition, its performance can degrade in the presence of weak interfering signals colliding with many of the pulses of the desired user [6]. In other words, since a BR completely ignores the information in the received signal samples with interference, it can lose useful information in the received signals as well, especially in weak interference scenarios. Therefore, in some cases, it can perform worse than the conventional matched filter detector, which is designed for single user cases and sets $\boldsymbol{\theta} = \mathbf{1}$ [26].

In order to achieve improved performance in the presence of weak interferers, the chip discriminator, which ignores only the signal samples with significant interference, can be used [27]. In that case, the weighting vector can be set as follows:

$$[\boldsymbol{\theta}]_j = \begin{cases} 1\,, & \text{if } \max\left\{\sqrt{E_2}\,\left|[\mathbf{s}_{1,j}]_2\right|, \ldots, \sqrt{E_K}\,\left|[\mathbf{s}_{1,j}]_K\right|\right\} < \tau_{\text{cd}} \\ 0\,, & \text{otherwise} \end{cases}, \tag{8.20}$$

where τ_{cd} is a threshold that is used to determine the significantly corrupted signal samples [25].

Quasi-decorrelator

Since an IR-UWB system can be regarded as a type of CDMA system, decorrelators can be employed to mitigate the effects of MAI [14]. A decorrelator is a linear detector that determines its weighting vector in order to cancel out MAI. In other words, it perfectly cancels out MAI in the absence of background noise; however, its performance degrades as the noise power increases [15]. The weighting vector calculation for a decorrelator requires the inversion of a $K \times K$ matrix. However, based on the simplified signal model in (8.16), which considers only the users that interfere with the desired user, a simplified version of the decorrelator, called quasi-decorrelator [14], can be defined by the following weighting vector

$$\boldsymbol{\theta} = \mathbf{S}_1\, \tilde{\mathbf{s}}_{\text{decor}}\,, \tag{8.21}$$

where $\tilde{\mathbf{s}}_{\text{decor}}$ represents the first column of $\left(\mathbf{S}_1^T \mathbf{S}_1\right)^{-1}$ with $\mathbf{S}_1$ denoting the signature matrix in (8.16).

It is noted that the quasi-decorrelator requires the inversion of a $(K_1 + 1) \times (K_1 + 1)$ matrix, where K_1 is the number of users interfering with the desired user. As studied in reference [14], the quasi-decorrelator can provide significant complexity reduction in some cases. However, its performance is practically equivalent to that of the BR, and degrades significantly when the number of users is large [6].

Quasi-MMSE detector

A decorrelator determines the weighting vector in order to cancel out MAI in the absence of noise. On the other hand, the conventional matched filter detector equally combines the received signal samples, which is the optimal approach in the absence of MAI. In the presence of both MAI and noise, the minimum mean-squared error (MMSE) detector provides an efficient mitigation of both effects [15]. Similar to the decorrelator, the MMSE detector requires the inversion of a $K \times K$ matrix. However, for IR-UWB systems, the simplified signal model in (8.16) can be used to obtain the quasi-MMSE detector [14], which is specified by the following weighting vector:

$$\boldsymbol{\theta} = \mathbf{S}_1 \, \tilde{\mathbf{s}}_{\text{mmse}} \, , \tag{8.22}$$

where $\tilde{\mathbf{s}}_{\text{mmse}}$ represents the first column of $\left(\mathbf{S}_1^T \mathbf{S}_1 + \sigma_n^2 (\mathbf{A}_1)^{-2}\right)^{-1}$.

When the main source of error is MAI, the quasi-MMSE detector and the quasi-decorrelator have similar performance. On the other hand, when the noise is the main source of error, the quasi-MMSE detector performs similarly to the conventional matched filter detector.

Optimal and suboptimal schemes for multipath channels

Although the linear detectors above are explained based on the simplified signal model in (8.16), high time resolution of UWB signals results in a large number of multipath components in practice. Therefore, IR-UWB receivers need to combine not only the signals in different frames but also the multipath components in each frame efficiently in order to achieve low error rates. To that aim, a Rake receiver as shown in Figure 8.2 can be employed to collect signal samples from M multipath components in each frame. It should be noted that since there are a large number L of multipath components in typical UWB channels, M is commonly smaller than L due to complexity constraints. Such Rake receivers that combine only a subset of the multipath components are called selective Rake receivers [28]. In a selective Rake receiver, it is important to optimally select M of the multipath components that are used at the receiver branches in Figure 8.2; this is called the finger selection problem [29]. After selecting the multipath components, it is also important to combine the signal samples optimally. In this part, it is assumed that finger selection has already been performed, and the aim is to obtain various linear detector structures with various performance and complexity.

Optimal linear MMSE detector First, the optimal linear detector for user 1 is obtained according to the MMSE criterion. Consider the received signal samples $r_{l,j}$ in (8.5) for

$l \in \mathcal{L} = \{l_1, \ldots, l_M\}$ and $j \in \{1, \ldots, N_f\}$, and let $\mathbf{r}$ represent an $N \times 1$ vector consisting of the distinct samples $r_{l,j}$ for $(l, j) \in \mathcal{L} \times \{1, \ldots, N_f\}$:

$$\mathbf{r} = \left[r_{l_1, j_1^{(1)}} \cdots r_{l_1, j_{m_1}^{(1)}} \cdots r_{l_M, j_1^{(M)}} \cdots r_{l_M, j_{m_M}^{(M)}} \right]^T , \tag{8.23}$$

where $\sum_{i=1}^{M} m_i = N$ denotes the total number of samples, with $N \leq MN_f$ [7]. From (8.5), $\mathbf{r}$ can be expressed as[1]

$$\mathbf{r} = \mathbf{SAb} + \mathbf{n} , \tag{8.24}$$

where $\mathbf{A}$ and $\mathbf{b}$ are as in (8.5) and $\mathbf{n} \sim \mathcal{N}(\mathbf{0}, \sigma_n^2 \mathbf{I})$. Also, $\mathbf{S}$ denotes a signature matrix, which has $\mathbf{s}_{l,j}^T$ in (8.7) for $(l, j) \in \mathcal{C}$ as its rows, where

$$\mathcal{C} = \left\{ \left(l_1, j_1^{(1)}\right), \ldots, \left(l_1, j_{m_1}^{(1)}\right), \ldots, \left(l_M, j_1^{(M)}\right), \ldots, \left(l_M, j_{m_M}^{(M)}\right) \right\} . \tag{8.25}$$

Based on (8.7)–(8.10), $\mathbf{S}$ can be expressed as $\mathbf{S} = \mathbf{S}^{(\mathrm{SP})} + \mathbf{S}^{(\mathrm{IFI})} + \mathbf{S}^{(\mathrm{MAI})}$. Then, after some manipulation, $\mathbf{r}$ becomes

$$\mathbf{r} = b^{(1)} \sqrt{\frac{E_1}{N_f}} (\boldsymbol{\alpha} + \mathbf{e}) + \mathbf{S}^{(\mathrm{MAI})} \mathbf{Ab} + \mathbf{n} , \tag{8.26}$$

where $\boldsymbol{\alpha} = \left[\alpha_{l_1}^{(1)} \mathbf{1}_{m_1}^T \cdots \alpha_{l_M}^{(1)} \mathbf{1}_{m_M}^T \right]^T$, with $\mathbf{1}_m$ denoting an $m \times 1$ vector of all ones, and $\mathbf{e}$ is an $N \times 1$ vector with elements $e_{l,j} = d_j^{(1)} \sum_{(n,m) \in \mathcal{A}_{l,j}} d_m^{(1)} \alpha_n^{(1)}$ for $(l, j) \in \mathcal{C}$ [7]. The received signal samples in (8.26) can also be expressed as the summation of the signal and the total noise terms as follows [7]:

$$\mathbf{r} = b^{(1)} \boldsymbol{\beta} + \mathbf{w}, \tag{8.27}$$

where

$$\boldsymbol{\beta} = \sqrt{\frac{E_1}{N_f}} (\boldsymbol{\alpha} + \mathbf{e}) , \tag{8.28}$$

$$\mathbf{w} = \mathbf{S}^{(\mathrm{MAI})} \mathbf{Ab} + \mathbf{n} . \tag{8.29}$$

For the signal model in (8.27), the optimal weights in (8.18) according to the MMSE criterion are given by

$$\boldsymbol{\theta} = \left(\boldsymbol{\beta}\boldsymbol{\beta}^T + \mathbf{R}_{\mathbf{w}} \right)^{-1} \boldsymbol{\beta} = c \, \mathbf{R}_{\mathbf{w}}^{-1} \boldsymbol{\beta} , \tag{8.30}$$

where $\mathbf{R}_{\mathbf{w}} = \mathrm{E}\{\mathbf{w}\mathbf{w}^T\}$ and $c = (1 + \mathrm{SINR})^{-1}$, with $\mathrm{SINR} = \boldsymbol{\beta}^T \mathbf{R}_{\mathbf{w}}^{-1} \boldsymbol{\beta}$ denoting the signal-to-interference-plus-noise ratio [15]. Note that the correlation matrix $\mathbf{R}_{\mathbf{w}}$ can be calculated from (8.29) for equiprobable symbols as

$$\mathbf{R}_{\mathbf{w}} = \mathbf{S}^{(\mathrm{MAI})} \mathbf{A}^2 \left(\mathbf{S}^{(\mathrm{MAI})} \right)^T + \sigma_n^2 \mathbf{I} . \tag{8.31}$$

It is noted from (8.30) and (8.31) that the calculation of the MMSE weighting vector requires the inversion of an $N \times N$ matrix, which can result in high computational

[1] The symbol index i is dropped from $\mathbf{b}_i$ for notational convenience.

complexity when the number of frames and/or the number of receiver branches (Rake fingers) is large [30].

Two-step MMSE detector In order to reduce the complexity of the linear MMSE detector specified by (8.18) and (8.30), a two-step MMSE combining approach can be considered [7]. In that case, the received signal samples $\mathbf{r}$ in (8.23) are first grouped into N_1 vectors as

$$\mathbf{r}_n = b^{(1)}\boldsymbol{\beta}_n + \mathbf{w}_n \ , \tag{8.32}$$

for $n = 1, \ldots, N_1$. Then, the samples in each group are combined according to the MMSE criterion via the following weighting vectors [30]:

$$\boldsymbol{\theta}_n = \left(\boldsymbol{\beta}_n\boldsymbol{\beta}_n^T + \mathbf{R}_{\mathbf{w}_n}\right)^{-1}\boldsymbol{\beta}_n = c_n\mathbf{R}_{\mathbf{w}_n}^{-1}\boldsymbol{\beta}_n \ , \tag{8.33}$$

where $c_n = (1 + \boldsymbol{\beta}_n^T\mathbf{R}_{\mathbf{w}_n}^{-1}\boldsymbol{\beta}_n)^{-1}$ and $\mathbf{R}_{\mathbf{w}_n} = \mathrm{E}\{\mathbf{w}_n\mathbf{w}_n^T\}$. In the second step, the combined samples, $\boldsymbol{\theta}_1^T\mathbf{r}_1, \ldots, \boldsymbol{\theta}_{N_1}^T\mathbf{r}_{N_1}$, are combined again according to the MMSE criterion. In order to formulate the second step, let $\hat{\mathbf{r}}$ denote the set of combined samples at the end of the first step; that is,

$$\hat{\mathbf{r}} = \left[\boldsymbol{\theta}_1^T\mathbf{r}_1 \ \cdots \ \boldsymbol{\theta}_{N_1}^T\mathbf{r}_{N_1}\right]^T \ , \tag{8.34}$$

which can be expressed as

$$\hat{\mathbf{r}} = b^{(1)}\hat{\boldsymbol{\beta}} + \hat{\mathbf{w}} \ , \tag{8.35}$$

with $\hat{\boldsymbol{\beta}} = [\boldsymbol{\theta}_1^T\boldsymbol{\beta}_1 \cdots \boldsymbol{\theta}_{N_1}^T\boldsymbol{\beta}_{N_1}]^T$ and $\hat{\mathbf{w}} = [\boldsymbol{\theta}_1^T\mathbf{w}_1 \cdots \boldsymbol{\theta}_{N_1}^T\mathbf{w}_{N_1}]^T$. Then, the symbol estimate is obtained as

$$\hat{b}^{(1)} = \mathrm{sgn}\left\{\boldsymbol{\gamma}^T\hat{\mathbf{r}}\right\} \ , \tag{8.36}$$

where $\boldsymbol{\gamma}$ is the MMSE weighting vector for the samples in $\hat{\mathbf{r}}$, which is calculated as

$$\boldsymbol{\gamma} = \left(\hat{\boldsymbol{\beta}}\hat{\boldsymbol{\beta}}^T + \mathbf{R}_{\hat{\mathbf{w}}}\right)^{-1}\hat{\boldsymbol{\beta}} = \hat{c}\,\mathbf{R}_{\hat{\mathbf{w}}}^{-1}\hat{\boldsymbol{\beta}} \ , \tag{8.37}$$

with $\mathbf{R}_{\hat{\mathbf{w}}} = \mathrm{E}\{\hat{\mathbf{w}}\hat{\mathbf{w}}^T\}$ [7]. It is noted from (8.33)–(8.37) that the two-step MMSE combining approach results in computational complexity reduction compared to the MMSE detector specified by (8.18) and (8.30). Specifically, it can be shown that the complexity of the former is $\mathcal{O}(N^{1.8})$ whereas it is $\mathcal{O}(N^3)$ for the latter [30]. This complexity reduction is accompanied by performance degradation in general, since each group ignores the information about the other groups in the first step of the two-step MMSE detector. However, whenever the noise samples in $\mathbf{w}_1, \ldots, \mathbf{w}_{N_1}$ of (8.32) are mutually uncorrelated, the two-step MMSE detector becomes the optimal linear detector, as discussed in reference [7]. In other words, the two-step MMSE detector is optimal when the correlation matrix $\mathbf{R}_{\mathbf{w}}$ in (8.31) has a block diagonal structure. When the correlation matrix does not have such a structure, grouping the highly correlated samples into the same group to obtain a "near block diagonal" structure can increase the performance of the two-step MMSE detector. To that aim, the following grouping algorithm is proposed in reference [7]:

1. $\mathcal{S} = \{1, \ldots, N\}$
2. for $i = 1 : N_1 - 1$
3. Choose a random sample s from $\mathcal{S}$
4. $\mathcal{S} = \mathcal{S} - \{s\}$
5. $\tilde{\mathcal{S}}_i = \{s\}$
6. for $j = 1 : \hat{N}_i - 1$
7. $\tilde{l} = \arg\max_{l \in \mathcal{S}} \sum_{k \in \tilde{\mathcal{S}}_i} |\rho_{lk}|$
8. $\tilde{\mathcal{S}}_i = \tilde{\mathcal{S}}_i \cup \{\tilde{l}\}$
9. $\mathcal{S} = \mathcal{S} - \{\tilde{l}\}$
10. $\tilde{\mathcal{S}}_{N_1} = \mathcal{S}$

where $\hat{N}_i$ denotes the number of samples in group i, for $i = 1, \ldots, N_1$, and the correlation coefficient ρ_{lk} is given by

$$\rho_{lk} = \frac{[\mathbf{R}_{\mathbf{w}}]_{lk}}{\sqrt{[\mathbf{R}_{\mathbf{w}}]_{ll}[\mathbf{R}_{\mathbf{w}}]_{kk}}} , \tag{8.38}$$

which is used as a measure for the level of correlation between any two samples. This low-complexity grouping algorithm begins with a random sample for each group, and then chooses the most correlated samples from the available index set $\mathcal{S}$ to form a group of highly correlated samples. Then, the resulting sets of indices $\tilde{\mathcal{S}}_1, \ldots, \tilde{\mathcal{S}}_{N_1}$ specify the groups of received signal samples to be combined in the first step of the two-step MMSE detector.

The idea behind the two-step MMSE detector can also be employed for multistep MMSE detectors. In other words, the received signal samples can be combined in more than two steps as well in order to achieve further reduction in computational complexity. However, performance degradation becomes more significant as the number of steps increases.

Optimal frame combining (OFC) detector In order to propose a two-step linear detector with lower computational complexity than the two-step MMSE detector, one can consider the OFC detector proposed in reference [31]. The OFC detector first combines the multipath components in each frame according to the maximal ratio combining (MRC) criterion, which is suboptimal in general, and then combines those combined samples in different frames according to the optimal linear MMSE criterion. Mathematically, the ith information symbol (bit) is estimated as

$$\hat{b}^{(1)} = \text{sign}\left\{ \sum_{j=iN_f}^{(i+1)N_f-1} \hat{\theta}_j \sum_{l \in \mathcal{L}} \alpha_l^{(1)} r_{l,j} \right\} , \tag{8.39}$$

where $\hat{\theta}_{iN_f}, \ldots, \hat{\theta}_{(i+1)N_f-1}$ are the MMSE weights for the ith bit, and $\mathcal{L} = \{l_1, \ldots, l_M\}$ represents the set of multipath components utilized at the receiver [31].

Optimal multipath combining (OMC) detector The OMC detector is the complement of the OFC detector in the sense that it combines, for each multipath component, the

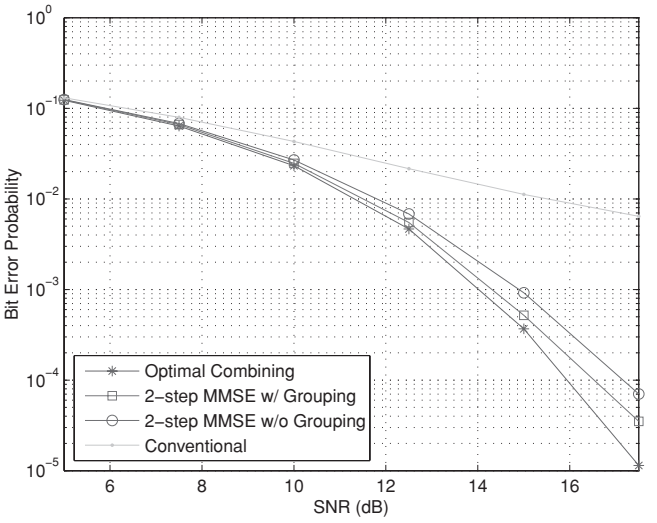

Figure 8.3 Bit error probability (BEP) versus signal-to-noise ratio (SNR) for the optimal, conventional, and two-step algorithms in a 5-user IR-UWB system over the channel, where $N_c = 10$, $N_f = 8$, $\mathcal{L} = \{1, 2, 3, 4\}$, and $E_k = 1\ \forall k$ (© 2006 IEEE) [30].

received signal samples from different frames suboptimally via equal gain combining (EGC), and then combines the combined samples for different multipath components according to the optimal linear MMSE criterion. In other words, the ith information bit is estimated as

$$\hat{b}^{(1)} = \text{sign}\left\{ \sum_{l \in \mathcal{L}} \tilde{\theta}_l \sum_{j=iN_f}^{(i+1)N_f - 1} r_{l,j} \right\}, \tag{8.40}$$

where $\tilde{\theta}_{l_1}, \ldots, \tilde{\theta}_{l_M}$ are the MMSE weights [31].

In order to compare the performance of the linear detectors studied in this section, consider the downlink of an IR-UWB system with five users ($K = 5$), where $E_k = 1\ \forall k$ [30]. The number of chips per frame, N_c, is equal to 10 and the discrete CIR is given by $\boldsymbol{\alpha}^{(k)} = [-0.4019\ 0.5403\ 0.1069 - 0.0479\ 0.0608\ 0.0005]\ \forall k$ [32]. The TH sequences and polarity codes of the users are selected from uniform distributions, and the results are averaged over different realizations. For the two-step MMSE detector, the numbers of samples in the groups are chosen to be equal. In the first scenario, $N_1 = 2$, $N_f = 8$, and $\mathcal{L} = \{1, 2, 3, 4\}$; i.e., only the first four multipath components are utilized at the receiver. Figure 8.3 illustrates the bit error probability (BEP) versus signal-to-noise ratio (SNR) for the optimal linear MMSE, the conventional,[2] and the two-step MMSE (with and without grouping) receivers. It is observed that the performance of the two-step MMSE receiver is close to that of the optimal linear MMSE receiver, and the conventional receiver, which combines the multipath components via MRC and the

[2] The conventional detector combines different multipath components via MRC and different frame components via EGC.

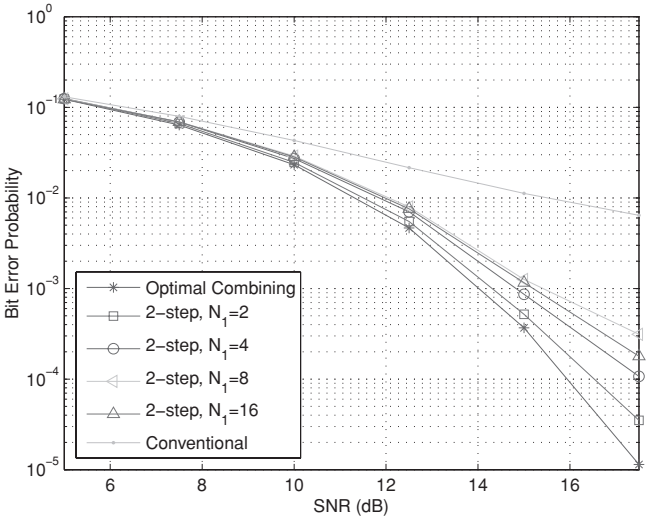

Figure 8.4 BEP versus SNR for the optimal, conventional, and two-step algorithms for various values of N_1, where the same parameters are used as in Figure 8.3 (© 2006 IEEE) [30].

frame components via EGC, has the worst performance. In addition, the advantage of grouping is observed for the two-step MMSE detector [30].

Next, the same parameters as in the previous scenario are considered, and the performance of the two-step MMSE detector with grouping is investigated for various numbers of groups, N_1, in Figure 8.4. As the number of groups increases, the algorithm gets more suboptimal due to the fact that the MMSE combining in each group ignores the information about the other groups. However, as N_1 gets close to N, which is 32 in this case, the detector starts performing better, since the MMSE combining in the second step becomes more effective (e.g., $N_1 = 16$ performs better than $N_1 = 8$). In fact, for $N_1 = N$, the two-step MMSE detector reduces to the optimal linear MMSE detector, since there occurs no combining in the first step since each group consists of a single sample in that case [7].

Finally, the performance of the two-step MMSE detector, the OMC detector, and the OFC detector is compared for $N_f = N_1 = 5$ and $\mathcal{L} = \{1, 2, 3, 4, 5\}$. Figure 8.5 shows that the two-step MMSE detector performs better than the OMC and OFC detectors as the optimal MMSE criterion is employed in both steps of the two-step MMSE detector whereas the OMC and OFC detectors employ EGC and MRC, respectively, in their first steps [7].

8.1.1.3 Iterative algorithms

Iterative MUD algorithms exchange soft information, in the form of posterior probabilities, between MUD and channel decoding units in order to provide low-complexity and near-optimal demodulation in coded multiple-access channels [6, 33]. This turbo principle of iteration among the two decision units, i.e., soft MUD and soft channel decoding, can also be used for IR-UWB systems that employ any kind of channel coding [34–38].

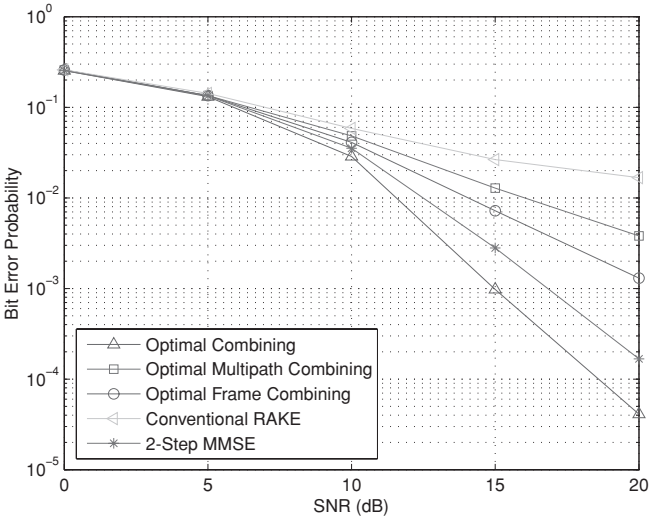

Figure 8.5 BEP versus SNR for the optimal, conventional, OMC, OFC, and two-step MMSE receivers, where $N_f = N_1 = 5$, $\mathcal{L} = \{1, 2, 3, 4, 5\}$, and all the other parameters are the same as in Figure 8.4 (© 2006 IEEE) [30].

In reference [35], a low-complexity iterative receiver is proposed for convolutionally coded IR-UWB systems, which is mainly composed of pulse correlators, soft interference canceler-likelihood calculators (SICLCs), soft-input soft-output (SISO) channel decoders, interleavers, and deinterleavers. The pulse correlator for user k correlates the received signal $r(t)$ with the received pulse $p_{\text{rx}}(t)$, and sends the correlation outputs to the SICLC unit. In the SICLC unit for user k, the total interference from all other users is calculated based on the soft information provided by the SISO channel decoders, and is subtracted from the correlation output corresponding to user k [6]. Then, based on the resulting output for user k, the log-likelihood ratio (LLR) for bit k is obtained by a single-user likelihood calculator [35]. That LLR forms the soft (extrinsic) information to be delivered to the kth SISO channel decoder, which uses it as the *a priori* information and calculates an update of LLRs for the coded bits based on the code constraint. Then, those updated LLRs are sent to the SICLC block for the next iteration. After a number of iterations, the bit decisions are obtained based on the LLRs calculated by the SISO channel decoders [6, 35].

Although the iterative multiuser detectors for CDMA systems can be applied to IR-UWB systems [34–38], iterative algorithms that exploit the special structure of IR-UWB signaling can result in low-complexity receivers [14, 39]. Specifically, iterative multiuser detectors can be designed for IR-UWB systems by regarding the IR-UWB signaling structure as a concatenated coding system, where the inner code is the modulation and the outer code is the repetition code. In reference [39], a low-complexity iterative receiver, called the pulse-symbol iterative detector, is proposed for IR-UWB systems over frequency selective channels. In order to describe this detector in more detail, let $\mathcal{L}^k = \{l_1^k, \ldots, l_M^k\}$, with $l_m^k \in \{1, 2, \ldots, L\}$ and $M \leq L$, denote the indices of the

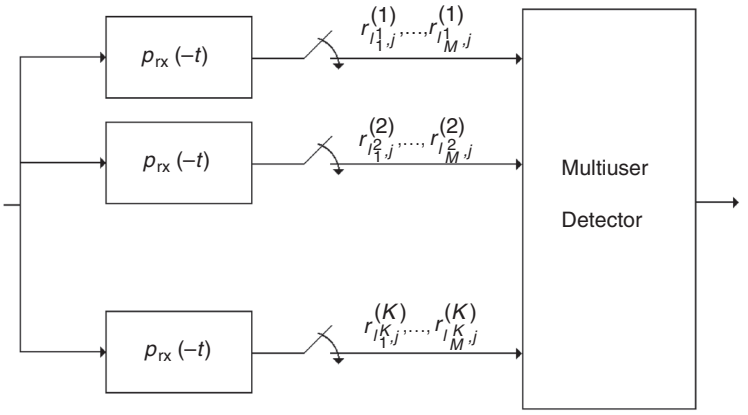

Figure 8.6 The general structure of the multiuser receiver in reference [39], where $p_{\text{rx}}(t)$ denotes the received UWB pulse.

signal paths the receiver samples for user k, and $r^{(k)}_{l,j}$ represent the received sample corresponding to the jth pulse of the kth user via the lth signal path (see Figure 8.6). In addition, the receiver combines the samples from the M multipath components in each frame via MRC for each user, and the resulting combined sample in the jth frame of user k is denoted by

$$\tilde{r}^{(k)}_j = \sum_{m=1}^{M} \alpha^{(k)}_{l^k_m} r^{(k)}_{m,j} \,, \tag{8.41}$$

where $\alpha^{(k)}_{l^k_m}$ is the channel coefficient for the l^k_mth path of user k. Based on the signal samples in (8.41), the pulse-symbol detector performs iterations between pulse detector and symbol detector stages in order to estimates the information symbols of the users [39].

Pulse detector In this stage, different pulses from the same user are assumed to correspond to independent information symbols. In other words, although it is known *a priori* that $b^{(k)}_{(i-1)N_f+1} = \cdots = b^{(k)}_{iN_f}$ for all $k \in \{1, \ldots, K\}$, the pulse detector ignores this information, where $b^{(k)}_j$ represents the information symbol carried by the jth pulse of the kth user. At the nth iteration, the pulse detector calculates the *a posteriori* LLR of $b^{(k)}_j$, given $\tilde{r}^{(k)}_j$ in (8.41), the information about the transmitted pulses from other users, and the *a priori* information about $b^{(k)}_j$ provided by the symbol detector, as [14]

$$L^n_1\left(b^{(k)}_j\right) \triangleq \log \frac{\Pr\left(b^{(k)}_j = 1 | \tilde{r}^{(k)}_j\right)}{\Pr\left(b^{(k)}_j = -1 | \tilde{r}^{(k)}_j\right)} \tag{8.42}$$

$$= \log \frac{f\left(\tilde{r}^{(k)}_j | b^{(k)}_j = 1\right)}{f\left(\tilde{r}^{(k)}_j | b^{(k)}_j = -1\right)} + \log \frac{\Pr\left(b^{(k)}_j = 1\right)}{\Pr\left(b^{(k)}_j = -1\right)} \tag{8.43}$$

for $j = 1, \ldots, N_f$ and $k = 1, \ldots, K$, where $f\left(\tilde{r}_j^{(k)} | \, b_j^{(k)} = i\right)$ is the likelihood of the jth combined sample for the kth user given that the transmitted symbol is equal to i. It is observed that the *a posteriori* LLR is the sum of the *a priori* LLR of the transmitted symbol,

$$\log \frac{\Pr\left(b_j^{(k)} = 1\right)}{\Pr\left(b_j^{(k)} = -1\right)} \triangleq \lambda_2^{n-1}\left(b_j^{(k)}\right) , \tag{8.44}$$

and the *extrinsic* information provided by the pulse detector about the transmitted symbol,

$$\log \frac{f\left(\tilde{r}_j^{(k)} | \, b_j^{(k)} = 1\right)}{f\left(\tilde{r}_j^{(k)} | \, b_j^{(k)} = -1\right)} \triangleq \lambda_1^{n}\left(b_j^{(k)}\right) . \tag{8.45}$$

Explicit expressions are provided in reference [39] for calculating the *a posteriori* LLR in (8.43).

Symbol detector The symbol detector utilizes the fact that $b_{(i-1)N_f+1}^{(k)} = \cdots = b_{iN_f}^{(k)}$ for all $k \in \{1, \ldots, K\}$. Therefore, it calculates the *a posteriori* LLR of $b_j^{(k)}$ given the extrinsic information from the pulse detector, and given $b_{(i-1)N_f+1}^{(k)} = \cdots = b_{iN_f}^{(k)}$ for all $k \in \{1, \ldots, K\}$, which results in the following expression [14]:

$$\begin{aligned} L_2^n\left(b_j^{(k)}\right) &\triangleq \log \frac{\Pr\left(b_j^{(k)} = 1 | \left\{\lambda_1^n\left(b_j^{(k)}\right)\right\}_{j=1,k=1}^{N_f,K} ; \text{constraints on pulses}\right)}{\Pr\left(b_j^{(k)} = -1 | \left\{\lambda_1^n\left(b_j^{(k)}\right)\right\}_{j=1,k=1}^{N_f,K} ; \text{constraints on pulses}\right)} \\ &= \underbrace{\sum_{i=N_f\lfloor (j-1)/N_f \rfloor + 1, i \neq j}^{N_f\lfloor (j-1)/N_f \rfloor + N_f} \lambda_1^n\left(b_i^{(k)}\right)}_{\lambda_2^n\left(b_j^{(k)}\right)} + \lambda_1^n\left(b_j^{(k)}\right) , \end{aligned} \tag{8.46}$$

where the constraints are $b_{(i-1)N_f+1}^{(k)} = \cdots = b_{iN_f}^{(k)}$ for every $k \in \{1, \ldots, K\}$. It is observed from (8.46) that the *a posteriori* LLR at the output of the symbol detector is the sum of the prior information from the pulse detector, $\lambda_1^n\left(b_j^{(k)}\right)$, and the extrinsic information about $b_j^{(k)}$, denoted by $\lambda_2^n\left(b_j^{(k)}\right)$, which is obtained from the information about all the pulses except for the jth pulse of the kth user. In the next iteration, this information is fed back to the pulse detector as *a priori* information on the jth pulse of the kth user [39].

The complexity of the pulse-symbol detector described above depends considerably on the number of pulses per information symbol, N_f. In some cases, an increase in N_f can increase the computational complexity significantly. Therefore, two low-complexity implementations are proposed in reference [39]. The first one is based on approximating

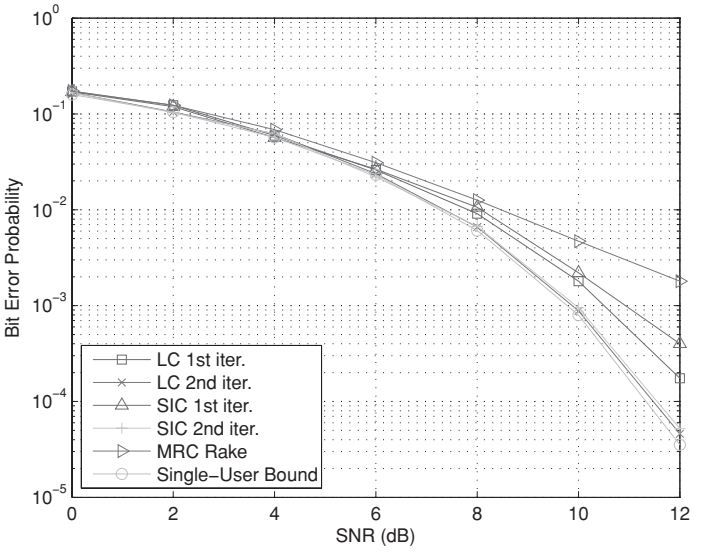

Figure 8.7 BEP versus SNR for various receivers (© 2008 IEEE) [39].

a part of the MAI by a Gaussian random variable, whereas the second one is based on soft interference cancelation. In Figure 8.7, the average probabilities of error are plotted versus SNR for both algorithms, where the labels "LC" and "SIC" correspond to the first and the second algorithms, respectively. In the simulations for Figure 8.7, 100 realizations of channel model 1 (CM-1) in the UWB indoor channel model reported by the IEEE 802.15.3a task group are used [40], and the uplink of a synchronous IR-UWB system with $N_f = 5$, $N_c = 250$, and a bandwidth of 0.5 GHz is considered. Also, the TH sequences are generated uniformly over $\{0, 1, \ldots, N_c - L - 1\}$ in order to prevent IFI [39]. In addition, a five-user environment is considered (i.e., $K = 5$), where the first user is assumed to be the user of interest. Each interfering user is modeled to have 10 dB more power than the user of interest so as to investigate an MAI-limited scenario. In all the receivers, the first 25 multipath components are employed; that is, $\mathcal{L}^1 = \{1, \ldots, 25\}$. It is observed from Figure 8.7 that the error rates of the proposed detectors are considerably lower than those of the MRC-Rake, which refers to the performance of a conventional MRC-Rake receiver as in reference [41]. In addition, just after two iterations, the performance of the proposed detectors gets very close to that of a single-user system. Furthermore, the low-complexity implementation based on the Gaussian approximation outperforms the low-complexity implementation based on soft interference cancelation after the first iteration, which is a price paid for the lower complexity of the latter algorithm. However, after two iterations, both detectors perform very closely to the single-user bound. As another example, the performance of the detectors that employ only the first five multipath components (that is, $\mathcal{L}^1 = \{1, 2, 3, 4, 5\}$) is investigated in Figure 8.8. The iterative detectors can still perform very closely to the single-user bound, whereas the MRC-Rake experiences an error floor [39].

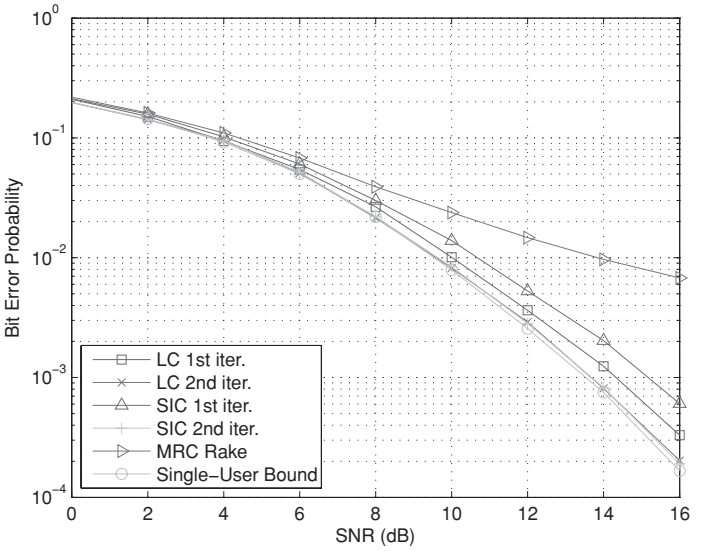

Figure 8.8 BEP versus SNR for various receivers (© 2008 IEEE) [39].

8.1.1.4 Other approaches for receiver design

In addition to the ML based, linear, and iterative detectors discussed above, the following approaches can also be employed for MAI mitigation in UWB systems:

Frequency domain approaches

Instead of processing the received signal samples in the time domain, one can take the Fourier transform of the signal samples, and perform MAI mitigation in the frequency domain as well [42–45]. In reference [42], an IR-UWB system that employs PPM is considered, and the Fourier transform of the received signal is taken by correlating the received signal with sinusoidal waveforms at different center frequencies. In this way, the problem of estimating the pulse positions in the time domain is converted into a phase estimation problem in the frequency domain, which results in a linear signal model. Then, typical linear detectors, such as the MMSE detector and the decorrelator, can be employed [6, 25]. The study in reference [43] extends the results in reference [42] to multipath channels. In addition, reference [45] proposes an ML detector in the frequency domain by exploiting the frequency correlation of MAI in direct sequence (DS) UWB systems.

Subspace approaches

Projection of a received signal vector onto a lower dimensional signal subspace can facilitate detector design with low computational complexity [25]. For example, the implementation of the optimal linear MMSE detector studied in Section 8.1.1.2 can be simplified by determining a low-rank subspace spanned by the columns of the covariance matrix. One way to achieve this rank-reduction is via principal component analysis [46, 47], which uses the eigen-decomposition of the covariance matrix to determine a

signal subspace spanned by the eigenvectors associated with the largest eigenvalues and a noise subspace spanned by the eigenvectors associated with the remaining eigenvalues. Then, the received signal vector is projected onto this signal subspace [6]. The application of this subspace approach to IR-UWB systems is studied in reference [48]. Another technique for rank-reduction is the multistage Wiener filter (MSWF) approach [49, 50], which does not require any eigen-decomposition, and commonly outperforms the other rank-reduction approaches [51].

Subtractive interference cancelation

In this approach, the aim is to estimate the MAI and to subtract it from the received signal [15, 16, 52]. One way of implementing this approach is to use successive interference cancelation, which estimates the interference due to each user and subtracts it from the received signal sequentially. In reference [53], successive interference cancelation is employed for UWB systems, by ranking the users according to their post-detection SNRs, and subtracting signal estimates sequentially (starting from the strongest user) from the received signal. Also, a partial Rake receiver is used to collect the energy of different multipath components [25]. Another study on subtractive interference cancelation for UWB system can be found in reference [54], which regenerates the interfering signals via a low-complexity partial Rake receiver. In addition to successive interference cancelation, the parallel interference cancelation approach detects all the signals in parallel and subtracts the interference *estimate* for each user (sum of all the signal estimates except for the desired user's) from the received signal. This procedure can be repeated a number of times in order to achieve improved performance, by using the results of the previous step to regenerate the interference [6]. Finally, the multistage detection and the decision feedback approaches can also be employed for MAI mitigation [15].

Blind approaches

For detectors that assume the knowledge of received signal parameters, such as the correlation matrix in (8.31), training sequences need to be used in practice in order to estimate those parameters before the detector can be implemented. On the other hand, *blind* detectors do not assume the knowledge of received signal parameters except for the signature vector and the timing of only the desired user and do not employ any training sequences [25, 55]. An example of the blind interference cancelation approach is the minimum variance (MV) detector, which aims to minimize the output variance with respect to a certain code-based constraint in order to estimate the desired user's signal while canceling the multiuser interference [56]. As another example, the *power of R* (POR) technique can be considered, which takes the power of the data covariance matrix to virtually increase the SNR [57]. In fact, the MV detector can be regarded as a special case of the POR detector [25].

8.1.2 Coding design for MAI mitigation

In the previous sections, MAI mitigation is achieved via various signal processing algorithms at the receiver. In this section, the effects of coding design on the mitigation

of MAI are investigated. In particular, the design of TH sequences and/or polarity codes in (8.1) is studied from a perspective of MAI mitigation.

8.1.2.1 Time-hopping sequence design

For synchronous IR-UWB systems over flat fading channels, it is possible to design N_c orthogonal TH sequences and to perform MAI-free communications, where N_c is the number of chips per frame in (8.1). Specifically, TH sequences can be chosen to satisfy $c_j^{(k_1)} \neq c_j^{(k_2)}$ for $k_1 \neq k_2$ and for all j. One way of designing orthogonal TH sequences is based on the use of congruence equations [25, 58, 59]. In particular, linear, quadratic, cubic, and hyperbolic congruence codes (LCC, QCC, CCC, and HCC) can be used for TH sequences in IR-IWB systems. For instance, a variant of linear congruence codes can be expressed as [58]

$$c_j^{(k)} = (k + j - 1)\, mod\, (N_c)\,, \tag{8.47}$$

for $j \in \{0, 1, \ldots, N_f - 1\}$ and $k \in \{1, \ldots, N_c\}$, where *mod* denotes the modulo operator. Based on the code construction technique in (8.47), it becomes possible to accommodate N_c orthogonal users in a synchronous IR-UWB system for flat fading channels [6].

Due to the high time resolution of UWB signals, IR-UWB systems commonly operate over frequency selective channels. Therefore, the TH sequence design techniques, such as that in (8.47), need to be generalized by considering the multipath characteristics of UWB channel channels. In references [60, 61], the following TH sequence design approach is proposed for synchronous IR-UWB systems over frequency selective environments:

$$c_j^{(k)} = \left((k-1)D + j + \left\lfloor \frac{k-1}{N_f} \right\rfloor \right) mod\ (N_c)\,, \tag{8.48}$$

for $j = 0, 1, \ldots, N_f - 1$ and $k = 1, 2, \ldots, N_c$, where $D = \lceil \tau_d / T_c + 1 \rceil$, with τ_d being the maximum excess delay, and $\lfloor . \rfloor$ and $\lceil . \rceil$ denoting the integer floor and integer ceiling operations, respectively. In addition, the number of pulses per symbol is selected as $N_f = N_c / D$ so that the multipath components do not destroy the orthogonal construction, and it is possible to perform MAI-free communications for $K \leq N_f$ [6].

In some applications, IR-UWB systems can have users with different numbers of pulses per information symbol in order to satisfy certain quality of service (QoS) requirements [62]. In other words, N_f in (8.1) can vary from user to user. In those scenarios, in order to facilitate the design of orthogonal TH sequences, one can consider a more general IR-UWB signaling structure, where the constraint of inserting pulses into certain frame intervals is removed [6, 60]. If $N_f^{(k)}$ denotes the number of pulses per information symbol of the kth user, a common symbol duration can be defined in terms of the chip duration as $N_c' = \sum_{k=1}^{K} N_f^{(k)}$. Then, the following TH sequence construction algorithm can be employed [60]:

1. for $k = 1 : K$
2. $\quad \mathbf{c}^{(k)} = \text{rand}(\mathcal{S}, N_f^{(k)})$
3. $\quad \mathcal{S} = \mathcal{S} - \mathbf{c}^{(k)}$
4. end

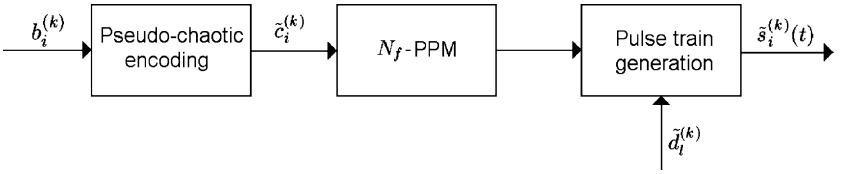

Figure 8.9 Block diagram of the transmitter for user k in a PCTH system.

where $\mathcal{S} = \{1, \ldots, N_c'\}$, $\mathbf{c}^{(k)} = \text{rand}(\mathcal{S}, N_f^{(k)})$ chooses $N_f^{(k)}$ random elements from the set $\mathcal{S}$ and inserts them into the vector $\mathbf{c}^{(k)}$, and $\mathcal{S} - \mathbf{c}^{(k)}$ denotes the exclusion of the elements of $\mathbf{c}^{(k)}$ from the set $\mathcal{S}$.

For scenarios in which the users' signals are not synchronized, it may not be possible to design orthogonal TH sequences. Then, the aim becomes designing TH sequences with good autocorrelation and cross-correlation properties. Due to the similarity between the design of time-hopping and frequency hopping codes, LCC, QCC, CCC, and HCC can be employed for IR-UWB systems [63]. The analysis in reference [60] indicates that QCC have reasonably good cross-correlation *and* autocorrelation characteristics compared to the other options [6].

8.1.2.2 Pseudo-chaotic time-hopping

Another approach for MAI mitigation via code design is the pseudo-chaotic time-hopping (PCTH) for IR-UWB systems [64]. In this approach, a pseudo-chaotic encoder driven by i.i.d. binary information symbols determines the frame (also called "slot") in which the pulses of a given user are transmitted. In addition, signature sequences specific to users are employed in order to mitigate the effects of MAI. A simplified block diagram of the transmitter for user k is illustrated in Figure 8.9. Specifically, the transmitted signal of user k for the ith information symbol is expressed as [65]

$$\tilde{s}_i^{(k)}(t) = \sum_{l=0}^{N_c-1} \tilde{d}_l^{(k)} p_{\text{tx}}\left(t - lT_c - \tilde{c}_i^{(k)} T_f\right), \qquad t \in [0, T_s), \tag{8.49}$$

where T_s is the symbol interval, which is divided into N_f frames each with duration T_f, the frame duration T_f consists of N_c chips (i.e., $T_f = N_c T_c$), $\tilde{d}_l^{(k)} \in \{0, 1\}$ is the signature for user k, and $\tilde{c}_i^{(k)} \in \{0, 1, \ldots, N_f - 1\}$ is the output of the pseudo-chaotic encoder that is determined by the incoming sequence of information bits. It is noted that each user transmits its pulses in one frame depending on the value of $\tilde{c}_i^{(k)}$, which is different from the conventional IR-UWB scheme in which each user transmits one pulse per frame. In a PCTH system, if two users transmit their pulses in different frames, there occurs no interference; however, if they send their pulses in the same frame, the pulses can overlap, but the effects of this overlap can be reduced by a careful design of the users' signature sequences $\tilde{d}_l^{(k)}$, for $l \in \{0, 1, \ldots, N_c - 1\}$, and $k = 1, \ldots, K$ [6].

In a typical PCTH system, the i.i.d. information bits are stored in an M-bit shift register, and the state of the system is represented by

$$x = 0.b_1 b_2 \ldots b_M = \sum_{i=1}^{M} 2^{-i} b_i, \tag{8.50}$$

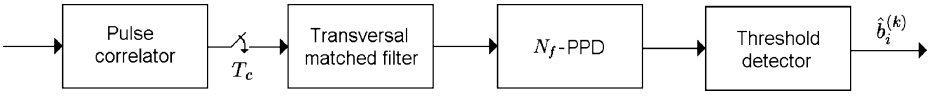

Figure 8.10 Block diagram of the receiver for user k in a PCTH system.

where $b_i \in \{0, 1\}$, and $x \in I = [0, 1]$. Dividing the interval I into $I_0 = [0, 0.5)$ and $I_1 = [0.5, 1]$, the binary information bits are assigned to different intervals, which implies that if a pulse is in the first half of a symbol interval, information 0 is being transmitted and if it is in the second half, a 1 is being transmitted. Dividing the symbol interval into $N_f = 2^M$ slots, the pulse can reside in any of the N_f positions in the symbol interval. For each new information bit, the binary bits in the representation of state x in (8.50) are shifted leftwards by discarding the old most significant bit (MSB), b_1, and assigning the new bit as the least significant bit (LSB), b_M [6, 64].

In Figure 8.10, a block diagram of the PCTH receiver is illustrated, which mainly consists of a pulse correlator, transversal matched filter, a pulse-position demodulator (PPD), and a threshold detector [66]. First, the received signal is correlated with the pulse shape and the correlator output is sampled at the chip rate. Then, the chip rate samples are fed into a digital transversal matched filter implemented by a tapped delay line [65]. After that, the PPD selects the largest sample among N_f samples at the output of the matched filter. Finally, the bit estimate is obtained via a threshold detector [66].

One of the advantages of IR-UWB systems with PCTH is the random distribution of inter-pulse intervals, which results in a smooth PSD of the transmitted signal. On the other hand, the main disadvantage is related to the self interference from the pulses of a given user, which can be significant in multipath channels, since all the pulses are transmitted in the same frame interval. In addition, the synchronization can be difficult since PCTH results in aperiodic TH sequences as the pulse positions depend on the incoming information symbols [6].

8.1.2.3 Multistage block-spreading (MSBS)

In a conventional IR-UWB system as in (8.1), each symbol is transmitted via N_f pulses, where each pulse resides in a frame interval of duration T_f that consists of N_c chips. For the TH sequence design studies in Section 8.1.2.1, the number of chips per frame, N_c, is considered as the upper limit on the number of users that can operate over flat fading channels without any MAI. However, the polarity codes, $d_j^{(k)}$ in (8.1) can also be utilized to increase the multiple-access capability of an IR-UWB system. In particular, the total processing gain of an IR-UWB system can be expressed $N_f N_c$, assuming UWB pulses with duration T_c, which implies a significantly larger multiuser capacity [67]. The multistage block-spreading (MSBS) approach in reference [9] utilizes this large user capacity of IR-UWB systems by means of polarity codes in addition to the TH sequences [6]. Therefore, it has the advantage of supporting many more active users compared to the approaches in the previous sections.

In the MSBS approach, when the total number of users satisfies $K \leq N_f N_c$, a TH sequence is assigned to a group of $\lfloor K/N_c \rfloor$ (or $\lceil K/N_c \rceil$) users. Then, the polarity codes

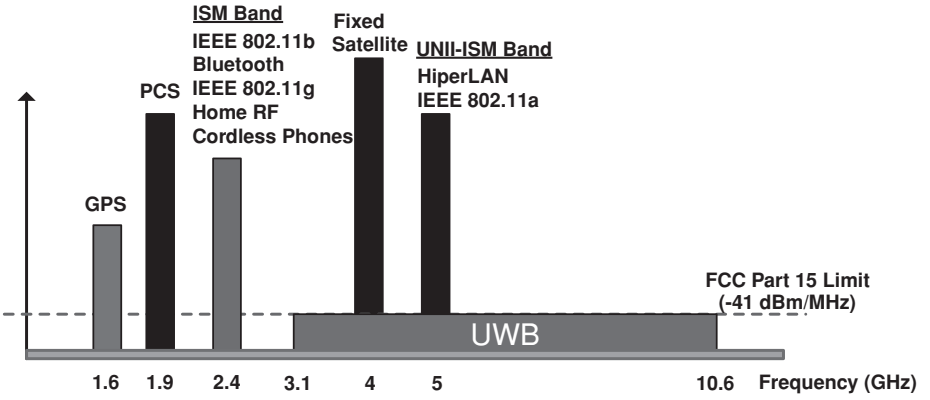

Figure 8.11 Spectrum crossover between narrowband and UWB systems.

(forming a "multiuser address") are used to distinguish among the users in the same group. In addition, the users in different groups are separated by their TH sequences. Therefore, the same polarity codes can be assigned to the users in different groups. By this joint use of the TH sequence and the polarity codes, $N_f N_c$ orthogonal user signals can be constructed [6, 9].

In an MSBS IR-UWB system, the transmitter first spreads a block of symbols, and then performs chip-interleaving. In this way, the mutual orthogonality between different users can be preserved even for multipath channels. At the receiver, the received signal is despread by a linear filtering stage, which essentially reduces the multiple-access channel into a set of single-user ISI channels. Then, an equalizer can be used for a given user before the symbol detection without any need for additional multiuser signal processing [6, 9].

8.2 Mitigation of narrowband interference (NBI)

UWB systems operate at a very low power over extremely wide frequency bands (wider than 500 MHz), where various narrowband (NB) technologies also operate with much higher power levels, as illustrated in Figure 8.11. Although NB signals interfere with only a small fraction of the UWB spectrum, due to their relatively high power with respect to the UWB signal, they might affect the performance and capacity of UWB systems considerably [68]. The recent studies show that the bit-error-rate (BER) performance of UWB receivers is greatly degraded due to the impact of NBI [69–74]. Therefore, either UWB transmitters should avoid transmission over the spectra of strong NB interferers, or UWB receivers should employ NBI suppression techniques to preserve the performance, capacity, and range of UWB communications.

NBI mitigation has been studied extensively for wideband systems such as direct sequence spread spectrum (DSSS)-based CDMA communications, and for broadband orthogonal frequency division multiplexing (OFDM) systems that operate in unlicensed

frequency bands. In CDMA systems, NBI is partially handled by the processing gain as well as by employing interference cancelation techniques. Approaches including notch filtering [75], linear and nonlinear predictive techniques [76–80], adaptive methods [81–84], MMSE detectors [85, 86], and transform domain techniques [87–91] are investigated extensively for interference suppression. NBI cancelation and avoidance in OFDM systems are studied in [92–95]. Compared to the cases of CDMA and OFDM, NBI suppression in UWB is a more challenging problem because of the restricted power transmission and the higher number of NB interferers due to the extremely wide bandwidth occupied by a UWB system. More significantly, in carrier modulated wideband systems, before demodulating the received signal both the desired wideband and the NB interfering signals are down-converted to the baseband, and the baseband signal is sampled at least with the Nyquist rate, which enables the use of various efficient NBI cancelation algorithms based on advanced digital signal processing techniques. In UWB, on the other hand, this kind of an approach requires a very high sampling frequency, which results in high power consumption and increases the receiver cost. In addition to the high sampling rate, the analog-to-digital-converter (ADC) must support a very large dynamic range to resolve the signal from the strong NB interferers. Currently, such ADCs are far from being practical. An alternative method to suppress NBI applied in wideband systems is to use analog notch filters. To be employed in UWB, this method requires a number of NB analog filter banks, since the frequency and power of the NB interferers can be various. Also, adaptive implementation of the analog filters is not straightforward. Therefore, employing analog filtering increases the complexity, cost, and size of UWB receivers. As a result, many of the NBI suppression techniques applied to other wideband systems are either not applicable to UWB, or the complexities of those methods are too high for the UWB receiver requirements.

In the remainder of this section, first, appropriate models for UWB and narrowband systems will be introduced. Later, techniques for avoiding NBI in UWB systems including multiband/multicarrier transmission and pulse shaping will be reviewed. Finally, some important NBI cancelation methods that might be applied to UWB systems will be addressed.

8.2.1 UWB and narrowband system models

It is necessary to investigate the models of the UWB signal and narrowband interferers for a thorough understanding of NBI effects on UWB systems. Considering a binary pulse position modulated (BPPM) IR-UWB signal, the transmitted waveform can be modeled as [96]

$$s(t) = \sum_{j=-\infty}^{\infty} p_{\text{tx}}(t - j\,T_{\text{f}} - c_j\,T_c - a\,\delta)\,, \tag{8.51}$$

where p_{tx} denotes the transmitted UWB pulse, T_{f} is the pulse repetition duration, c_j is the TH code in the jth frame, T_c is the chip time, δ is the pulse position offset regarding BPPM, and a represents the data, which is a binary number.

Depending on its type, the NBI can be modeled in various ways. For example, it can be considered to consist of a single tone interferer, which can be modeled as

$$i(t) = \gamma\sqrt{2P}\cos(2\pi f_c t + \phi_i)\,, \tag{8.52}$$

where γ is the channel gain, P is the average power, f_c is the frequency of the sinusoid, and ϕ is the phase.

NBI can also be thought of as the effect of a band limited interferer, then the corresponding model is a zero-mean Gaussian random process, and its PSD is as follows:

$$S_i(f) = \begin{cases} P_{\text{int}}\,, & f_c - \frac{B}{2} \le |f| \le f_c + \frac{B}{2} \\ 0\,, & \text{otherwise} \end{cases}\,, \tag{8.53}$$

where B, f_c, and P_{int} are the bandwidth, center frequency, and PSD of the interferer, respectively.

Since the NB signal has a bandwidth much smaller than the coherence bandwidth of the channel, the time domain samples of the NBI are highly correlated with each other. Therefore, for the investigation of the NB interferers, the correlation functions are of primary interest, rather than the time- or frequency domain representations. The correlation functions corresponding to the single tone and band-limited cases can be written as

$$R_i(\tau) = P_i|\gamma|^2\cos(2\pi f_c\tau)\,, \tag{8.54}$$

$$R_i(\tau) = 2P_{\text{int}}B\cos(2\pi f_c\tau)\,\text{sinc}(B\tau)\,, \tag{8.55}$$

respectively. The resulting correlation matrices for the kth and lth interference samples are [97]

$$[\mathbf{R}_i]_{k,l} = 4N_s P_i|\gamma|^2|W_r(f_c)|^2\left[\sin(\pi f_c\delta)\right]^2\cos\left(2\pi f_c(\tau_k - \tau_l)\right) \tag{8.56}$$

for the single tone interferer, and

$$\begin{aligned}[\mathbf{R}_i]_{k,l} = {} & 2N_s P_{\text{int}}B|W_r(f_c)|^2 \\ & \times\Big[\,2\cos\left(2\pi f_c(\tau_k - \tau_l)\right)\text{sinc}\left(B(\tau_k - \tau_l)\right) \\ & -\cos\left(2\pi f_c(\tau_k - \tau_l - \delta)\right)\text{sinc}\left(B(\tau_k - \tau_l - \delta)\right) \\ & -\cos\left(2\pi f_c(\tau_k - \tau_l + \delta)\right)\text{sinc}\left(B(\tau_k - \tau_l + \delta)\right)\Big]\end{aligned} \tag{8.57}$$

for the case of band-limited interference, where $|W_r(f_c)|^2$ is the PSD of the received signal at the frequency f_c.

Another strong candidate for UWB communications besides the impulse radio is the multicarrier approach, which can be implemented using OFDM. OFDM has become a very popular technology for wireless communications due to its special features such as robustness against multipath interference, ability to allow frequency diversity with the use of efficient forward error correction (FEC) coding, and ability to provide high bandwidth efficiency. A strong motivation for employing OFDM in UWB applications is its resistance to NBI, and its ability to turn the transmission *on* and *off* on separate

subcarriers depending on the level of interference. The NBI models that can be considered for OFDM include one or more tone interferers, as well as a zero-mean Gaussian random process that occupies certain subcarriers along with white noise as

$$S_n(\kappa) = \begin{cases} \frac{N_i+N_w}{2}, & \text{if } \kappa_1 < \kappa < \kappa_2 \\ \frac{N_w}{2}, & \text{otherwise} \end{cases}, \tag{8.58}$$

where κ is the subcarrier index, κ_1 is the index of the first occupied subcarrier, κ_2 is the index of the last occupied subcarrier, and $N_i/2$ and $N_w/2$ are the spectral densities of the narrowband interferer and white noise, respectively.

8.2.2 NBI avoidance

NBI can be avoided at the receiver by properly designing the transmitted UWB waveform. If the statistics of NBI are known, the transmitter can adjust the transmission parameters appropriately. NBI avoidance can be achieved in various ways, and it depends on the type of access technology.

8.2.2.1 Multi-carrier approach

The multi-carrier approach can be one way of avoiding NBI. OFDM, which was mentioned in the previous section, is a well-known example for multi-carrier techniques. In OFDM-based UWB, NBI can be avoided easily by an adaptive OFDM system design. Since NBI will corrupt only some subcarriers in the OFDM spectrum, only the information transmitted over those frequencies will be affected from the interference. If the interfered subcarriers can be identified, transmission over those subcarriers can be avoided. In addition, by sufficient FEC and frequency interleaving, jamming resistance against NBI can also be obtained.

At the OFDM receiver, the signal is received along with noise and interference. After synchronization and removal of the cyclic prefix, FFT is applied to convert the time-domain received samples to the frequency domain signal. The received signal at the κth subcarrier of the mth OFDM symbol can then be written as

$$Y_{m,\kappa} = S_{m,\kappa} H_{m,\kappa} + \underbrace{I_{m,\kappa} + W_{m,\kappa}}_{\text{NBI+AWGN}}, \tag{8.59}$$

where $S_{m,\kappa}$ is the transmitted symbol which is obtained from a finite set (e.g., QPSK or QAM), $H_{m,\kappa}$ is the value of the channel frequency response, $I_{m,\kappa}$ is the NBI, and $W_{m,\kappa}$ denotes the uncorrelated Gaussian noise samples.

In OFDM, in order to identify the interfered subcarriers, the transmitter requires a feedback from the receiver. The receiver should have the ability to identify those interfered subcarriers. Once the receiver estimates those subcarriers, the relevant information will be sent back to the transmitter. The transmitter will then adjust the transmission accordingly. Note that in such a scenario, the interference statistics need to be constant for a certain period of time. If the interference statistics change rapidly, by the time the transmitter receives feedback, and adjusts the transmission parameters, the receiver might observe different interference characteristics.

The feedback information can be various, including the interfered subcarrier index, in some cases the amount of interference on these subcarriers, and the center frequency and the bandwidth of the NBI. The identification of the interfered subcarriers can also be various. One simple technique is to look at the average signal power in each subcarrier, and to compare it against a threshold. If the average received signal power of a subcarrier is larger than the threshold, that channel can be regarded as severely interfered by NBI.

8.2.2.2 Multiband schemes

Similar to the multicarrier approach, multiband schemes are also considered for avoiding NBI. Rather than employing a UWB radio that uses the entire 7.5 GHz band to transmit information, the spectrum can be divided into smaller subbands by exploiting the flexibility of the FCC definition of the minimum bandwidth of 500 MHz [17]. The combination of these subbands can be used freely for optimizing the system performance. By splitting the spectrum into smaller chunks that are still larger than 500 MHz, NBI can be avoided, and better coexistence with other wireless systems can be achieved. A multiband approach will also enable worldwide inter-operability of the UWB devices, as the spectral allocation for UWB could possibly be different in different parts of the world. In multiband systems, information on each of the subbands can be transmitted using either single-carrier (pulse-based) or multicarrier (OFDM) techniques.

8.2.2.3 Pulse shaping

Another technique for avoiding NBI is pulse shaping. As can be seen in (8.56) and (8.57), the effect of interference is directly related to the spectral characteristics of the receiver template pulse waveform. That means that, if the transmission at the frequencies where NBI is present can be avoided, the influence of interference on the received signal can be mitigated significantly. Therefore, designing the transmitted pulse shape properly, such that the transmission at some specific frequencies is omitted, NBI avoidance can be realized. An excellent example for the implementation of this approach is the Gaussian doublet [98]. A Gaussian doublet, representing one bit, consists of a pair of narrow Gaussian pulses with opposite polarities. Considering the time delay T_{d} between the pulses, the doublet can be represented as

$$s_d(t) = \frac{1}{\sqrt{2}} \left(s(t) - s(t - T_{\mathrm{d}}) \right) . \tag{8.60}$$

The corresponding spectral amplitude of the doublet is then

$$|S_d(f)|^2 = 2|S(f)|^2 \sin^2(\pi f T_{\mathrm{d}}) , \tag{8.61}$$

where $|S(f)|^2$ is the power spectrum of a single pulse. It is noted that due to the sinusoidal term in (8.61), the power spectrum has nulls at $f = n/T_{\mathrm{d}}$, where n can be any integer (see Figure 8.12). The basic idea for avoiding NBI is to adjust the location of these nulls in such a way that they overlap with the peaks created by narrowband interferers. By modifying the time delay T_{d}, a null can be obtained at the specific frequency where NBI exists, and in this way the strong effect of the interferer can be avoided. If T_{d} is adjusted

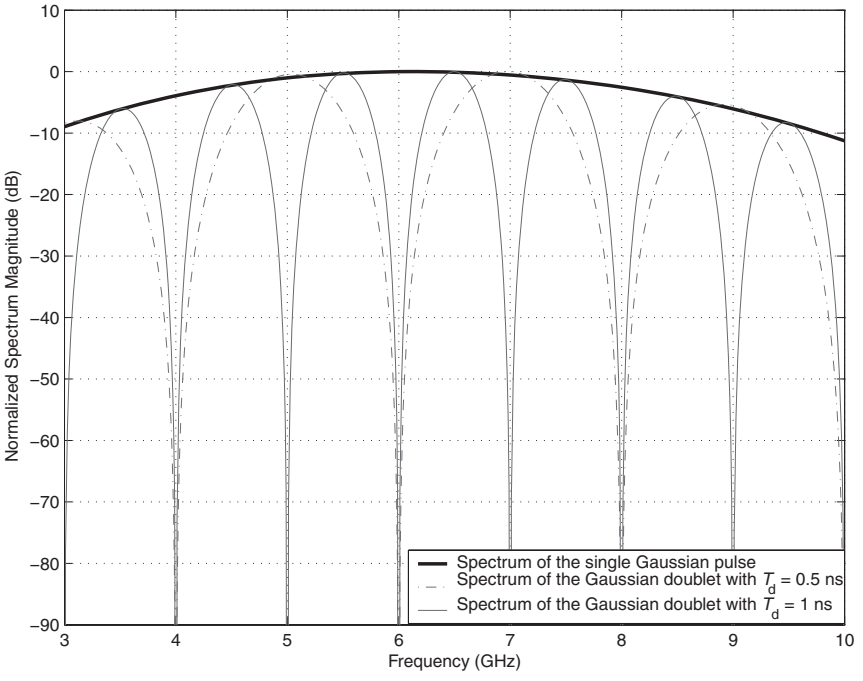

Figure 8.12 Normalized spectra for the single Gaussian pulse and two different Gaussian doublets.

to 0.5 ns, for example, the interferers located at the integer multiples of 2 GHz can be suppressed.

The purpose of avoiding NBI through abstaining transmission at frequencies of interference can also be carried out by making use of notch filters in the transmitter. To accomplish this, the parameters of the filters have to be adjusted such that the notches they create overlap with the frequencies of strong NBI. When notch filters are employed in the transmitter, the transmitted pulse is shaped in such a way (see Figure 8.13) that the correlation of the NBI with the pulse template in the receiver is minimized.

Pulse-shaping techniques are not limited to the Gaussian doublet and notch filtering. Another feasible method is the adjustment of the PPM modulation parameter δ in (8.51). Revisiting the correlation matrix for a single tone interferer given in (8.56), it is seen that $[\mathbf{R}_i]_{k,l} = 0$ for $\delta = n/f_c$, where $n = 1, 2, \ldots, M$, with M being the number of possible pulse positions. Therefore, an effective interference avoidance can be attained by setting δ to n/f_c. Similarly, considering the correlation matrix corresponding to the band-limited interference (8.57), it is seen that $\cos(2\pi f_c(\tau_k - \tau_l \pm \delta)) = \cos(2\pi f_c(\tau_k - \tau_l))$, when $\delta = n/f_c$. Also, in the light of the knowledge that the bandwidth of the interference (B) is much smaller than its center frequency (f_c), the assumption $\text{sinc}(B(\tau_k - \tau_l \pm \delta)) \simeq \text{sinc}(B(\tau_k - \tau_l))$ can be made for $\delta = n/f_c$. These two facts lead to the conclusion that $[\mathbf{R}_i]_{k,l}$ in (8.57) becomes zero for the band-limited interference case, too, when δ is set to n/f_c.

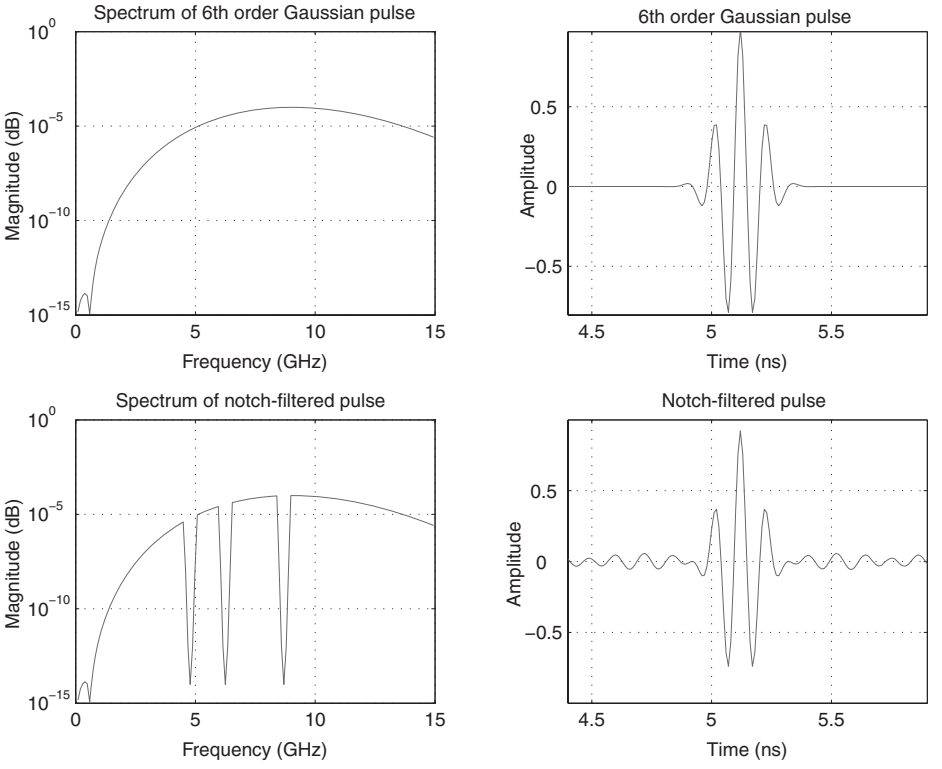

Figure 8.13 The effect of notch filtering on the transmitted pulse shape.

Although the adjustment of the PPM modulation parameter δ is a straightforward way of avoiding NBI, it has an important drawback. The correlation output is also dependent on δ, and for a certain value of it a maximum signal correlation can be obtained. However, this value of δ does not necessarily have to be equal to $1/f_c$. For the AWGN case (without considering the NBI), the BER function from which the optimum δ can be determined is [99]

$$Q\left(\sqrt{\frac{N_s A E_p}{N_0} R_{\text{opt}}}\right), \tag{8.62}$$

where $R_{\text{opt}} = R(0) - R(\delta_{\text{opt}})$, N_s is the number of pulses per symbol, A is the pulse amplitude, $N_0/2$ is the double sided PSD of AWGN, and $R(\Delta t)$ is the autocorrelation function of the received pulse. Therefore, there is an obvious tradeoff between maximizing R_{opt} and avoiding NBI, when determining the δ parameter. Depending on the level of NBI and AWGN, this parameter can be adjusted to provide an optimal performance.

8.2.2.4 Other NBI avoidance methods

For the IR-UWB systems, it is possible to avoid NBI by placing notches in the spectrum via adjusting the TH code [100]. In reference [101], a PAM UWB signal is considered. Each symbol has a duration of T_s and is composed of N_f pulses, giving rise to N_f

frames, which last for $T_f = T_s/N_f$ and are divided into chips with a duration of T_c. The pseudo-random TH code determines the position of the pulse inside the frame by selecting the chip where to place the pulse. In short, a PAM UWB signal over a symbol duration can be written as

$$u(t) = A \sum_{n=0}^{N_f-1} p_{\text{tx}}(t - c_n T_c - n T_f - T_s) \,, \tag{8.63}$$

where $A \in \{-1, 1\}$ denotes the amplitude of the pulse, and c_n is the TH code. In reference [100], the spectrum shape for the multisymbol case is given by

$$P_u(f) = |W(f)|^2 \sum_{m=0}^{N_b-1} |T_m(f)|^2 \,, \tag{8.64}$$

where $W(f)$ is the Fourier transform of the transmitted pulse $p_{\text{tx}}(t)$, N_b is the total number of different TH codes used, m is the symbol index, and

$$T_m(f) = \sum_{n=0}^{N_f-1} \exp\left\{-j2\pi f(c_{n,m} T_c + n T_f + m T_s)\right\} \,. \tag{8.65}$$

From (8.65), it is observed that changing the TH code causes the spectrum of the transmitted signal to vary. This means that by employing various methods, the TH code can be adjusted in such a way that spectral notches are created at the frequencies of strong NB interferers, allowing the system to avoid NBI.

In addition to the methods mentioned above, physical solutions can also be considered for avoiding NBI. In reference [102], an NBI avoidance technique based on antenna design is proposed. The main idea is to generate frequency notches by intentionally adding a narrowband resonant structure to the antenna, and thus, make it insensitive to some particular frequencies. This technique is more economical than the explicit notch-filtering method, since it does not require additional notch filters. In reference [102], a frequency notched UWB antenna suitable for avoiding NBI is realized and explained in detail. This special-purpose antenna is obtained by employing planar elliptical dipole antennas and incorporating a half-wave resonant structure, which is obtained by implementing triangular and elliptical notches. It is important to note that the performance of the antenna is reduced as the number of notches increases. This fact leads to the idea that the frequency notched antenna may not be successful enough in avoiding numerous simultaneously existing NB interferers.

8.2.3 NBI cancelation

Although most of the avoidance methods mentioned seem to have high feasibility, they may not be implemented under all circumstances. The main limitation on those methods is their dependency on the exact knowledge about NB interferers. Without having the accurate information about the center frequency of the interference, suppressing NBI is not possible by means of any of the avoidance techniques explained. Even if the complete knowledge about the NBI is available, if there is an abundant number of

interferers, methods such as employing notch filters or changing the parameters of the transmitted pulse may lose their practicality. If it is not possible to avoid NBI at the transmission stage for any reason, one should make an effort at the receiver side for extracting and eliminating it from the received signal.

Throughout the previous section, the methods for avoiding NBI were discussed and the limitations on their realization were mentioned. In practice, UWB systems that employ only avoidance techniques are not totally successful in eliminating NBI. In this section, an overview of different types of NBI cancelation method will be provided.

8.2.3.1 MMSE combining

One of the popular receivers considered for UWB is the Rake receiver. Rake receivers are designed to collect the energy of strong multipath components, and with this purpose they employ *fingers* [28,29]. At each Rake finger, there is a correlation receiver synchronized with one of the multipath components. The correlation receiver is followed by a linear combiner whose weight is determined depending on the combination algorithm used. The output of the receiver for the ith pulse can be denoted as [103]

$$y_i = \sum_{l=0}^{L_f-1} (a_i \theta_l \psi \beta_l + \theta_l n_l) \ , \tag{8.66}$$

where L_f is the number of Rake fingers, a_i is the data bit transmitted on the ith pulse, θ_l, β_l, and n_l are the weight used by the combiner, the channel gain, and the noise for the lth multipath component, respectively, and

$$\psi = \int_{-\infty}^{\infty} p_{\text{rx}}(t) v(t) dt \ , \tag{8.67}$$

with $p_{\text{rx}}(t)$ denoting the received waveform, and $v(t)$ being the correlating function.

In the traditional Rake receiver, which employs MRC, the weight of the combiner is the conjugate of the gain of the particular multipath component ($\theta_l = \beta_l^*$). Such a selection maximizes the SNR in the absence of NBI. However, when NBI exists, MRC is no longer the optimum method as the interference samples are correlated. The MMSE combining, which is an alternative approach, depends on varying these weights in such a way that the mean-squared error between the required and actual outputs is minimized. The MMSE weights are calculated as [104]

$$\boldsymbol{\theta} = k \mathbf{R}_n^{-1} \boldsymbol{\beta} \ , \tag{8.68}$$

where $\boldsymbol{\theta} = [\theta_1 \ \theta_2 \ \cdots \ \theta_M]^T$, k is a scaling constant, $\mathbf{R}_n^{-1}$ is the inverse of the correlation matrix of the noise-plus-interference term, and $\boldsymbol{\beta} = [\beta_1 \ \beta_2 \ \cdots \ \beta_M]^T$ is the channel gain vector.

The NBI cancelation methods other than MMSE combining can be grouped into three categories as frequency domain, time-frequency domain, and time-domain approaches.

8.2.3.2 Frequency domain techniques

Cancelation techniques in the frequency domain can be exemplified by notch filtering in the receiver side. Having an estimate of the frequencies of the powerful NB interferers,

notch filters can be used to suppress NBI. The appealing fact about this method is that it can be utilized in almost all kinds of receiver, so that the UWB system is not forced to employ a correlation-based receiver. The main weakness of the frequency domain methods, on the other hand, is that they are useful only when the received signal, which is a superposition of the UWB signal and NBI from various sources, exhibits stationary behavior. If the received signal has a time-varying nature, methods that analyze the frequency content taking the temporal changes into account are required. These methods are called the time-frequency approaches.

8.2.3.3 Time-frequency domain techniques

The most commonly employed time-frequency domain method for interference suppression is the wavelet transform. Similar to the well-known Fourier transform, the wavelet transform also employs basis functions, which are called wavelets. A wavelet is defined as

$$\psi_{a,b}(t) = \frac{1}{|\sqrt{a}|}\,\psi\left(\frac{t-b}{a}\right)\,, \tag{8.69}$$

where a and b are the scaling and shifting parameters, respectively. If these parameters are set as $a = 1$ and $b = 0$, the mother wavelet is obtained. By dilating and shifting the mother wavelet, a family of daughter wavelets is formed. The continuous wavelet transform can be expressed as

$$W(a,b) = \int_{-\infty}^{+\infty} f(t)\psi_{a,b}(t)dt\,. \tag{8.70}$$

One possible way of suppressing NBI via the wavelet transform is to have the transmitter part of the UWB system estimate the electromagnetic spectrum, and set a proper threshold for interference detection [105]. The interference level at each frequency component is then determined with the wavelet transform, and compared to this threshold in order to distinguish between the interfered and not interfered frequency components. According to the results of this comparison step, the transmitter does not transmit at frequencies where strong NBI exists. Obviously, this method is quite similar to the multicarrier approach in the NBI avoidance techniques.

Methods employing the wavelet transform in the receiver side of the system also exist [106, 107]. In these methods, the wavelet transform is applied to the received signal, and the frequency components with considerably high energy are considered to be affected by the NBI. These components are then suppressed by using conventional methods such as notch filtering.

8.2.3.4 Time-domain techniques

Time-domain approaches, which can also be called predictive methods, are based on the assumption that the predictability of narrowband signals is much higher than the predictability of wideband signals, because wideband signals have a nearly flat spectrum [108]. Hence, in a UWB system, a prediction of the received signal is expected to

primarily reflect the NBI rather than the UWB signal. This fact leads to the consequence that NBI can be canceled by subtracting the predicted signal from the received signal.

Predictive methods can be classified as linear and nonlinear techniques. Linear techniques employ transversal filters in order to get an estimate of the received signal depending on the previous samples and model assumptions [79]. If one-sided taps are used, the filter employed is a linear prediction filter, whereas it is a linear interpolation filter if the taps are double-sided. It is worth noting that interpolation filters prove to be more effective in canceling NBI.

Common examples for linear predictive methods are the Kalman–Bucy prediction, which is based on the Kalman–Bucy filter with infinite impulse response (IIR), and the least-mean-squares (LMS) algorithm based on a finite impulse response (FIR) structure.

Nonlinear methods are found to provide a better solution than linear ones for DS systems because they are able to make use of the highly non-Gaussian structure of the DS signals [108]. However, for UWB systems, this is not the case since such a non-Gaussianity does not exist in UWB signals.

Adaptive prediction filters are considered as a powerful tool against NBI. When an interferer is detected in the system, the adaptation algorithm creates a notch to suppress the interference caused by this source. However, if the interferer vanishes suddenly, since there is no mechanism to respond immediately to remove the notch created, the receiver continues to suppress the portion of the wanted signal around the notch. If NB interferers enter and exit the system in a random manner, this shortcoming reduces the performance of the adaptive system dramatically. A more useful algorithm is proposed in reference [79], where a hidden Markov model (HMM) is employed to keep track of the interferers entering and exiting the system. In this algorithm, the frequency locations where an interferer is present are detected by an HMM filter, and a suppression filter is inserted there. When the system detects that the interferer has vanished, the filter is removed automatically.

8.3 Interference awareness

Up until this point, interference in UWB systems has been investigated from the mitigation perspective, especially in a multiuser environment. In order to focus on interference awareness, a broader definition of interference might be necessary. In this way, the discussion outlined here can also be related to other wireless communications domains such as next generation wireless networks (NGWNs) and cognitive radios (CRs). In this sense, interference can be defined as any kind of signal received besides the desired signal and noise. Interference may occur in the following two ways depending on its source:

1. *Self-interference*, which is caused by the own transmitted signal due to improper system design or adverse channel conditions.
   Examples include ISI, inter-carrier interference (ICI), IFI, inter-pulse interference (IPI), and cross-modulation interference (CMI). Self-interference can be handled by properly designing the system and transceivers.

2. *Interference from other users*, which can be further categorized as
   - Multiuser interference, which is the interference from users using the same system or a similar technology. Co-channel interference (CCI) and adjacent channel interference (ACI) belong to this category. It can be overcome by proper multiaccess design and/or employing multiuser detection techniques.
   - Interference from other types of technology, a sort of interference that mostly requires interference avoidance or cancelation. It is more difficult to handle compared to multiuser interference and often it cannot be suppressed completely. NBI is a well-known example of this type of interference.

Among the two types of interference listed above, the latter one (and especially CCI) draws more attention especially with the increasing demand and services in wireless communications. Note that, by being slightly different from UWB systems, NGWNs focus on frequency reuse of one (FRO) scheme in order to avoid arduous and expensive systemwise planning step due to the underutilization concern of the electromagnetic spectrum. However, FRO comes at the expense of dramatic CCI levels, especially for the user equipments (UEs) in the vicinity of cell borders. This fact obligates nodes in NGWNs and CR systems to be aware of many factors influencing interference to perform better under such conditions.

In order to establish a framework for interference awareness, factors affecting CCI can be investigated from the perspective of the traditional protocol stack. Yet, there are some factors that affect CCI but cannot be populated in any of the layers, since they cannot be measured (therefore, controlled) in real-time in an adaptive manner. Weather and seasonal variations would be one of the most interesting "non-layer factors" influencing interference and falling into this category. Due to the presence of high-pressure air, signals can sometimes be reflected to the distances to which they are not intended [109, 110] (for related models such as two-ray ground reflection model, see reference [110, Section 3]). Since the signal over the same channel is able to reach the other terminal, CCI inevitably occurs. Especially for UWB systems, one of the most interesting instances of such a nonlayered factor is the impact of extreme humidity, other gaseous media, or even water in liquid form (such as in an office where a fire alarm goes off and sprinklers spray water) present in the propagation environment. As can be predicted, the attenuation characteristics of UWB signals change drastically depending on the environmental properties which imply different interference behaviors [111].

Since wireless propagation is governed by the physical environment, namely by topographical and even by demographical characteristics (and by the traffic distribution which depends also on the same two factors [112, 113] indirectly), it can be concluded that CCI is affected by the physical environment as well. However, it is very difficult to model those effects, since they are mathematically intractable. Statistically speaking, one can still observe more severe interference levels in urban areas due to the large number of base stations and mobiles [114, and references therein]. In indoor environments, depending on the use of devices, CCI is more likely to occur, since there are many devices (e.g., microwave ovens and telephone handsets) operating in the similar bands. Especially in indoor environments, in conjunction with propagation channel

properties, interference conditions change depending on the propagation characteristics since non-line-of-sight (NLOS) cases experience more severe interference compared to line-of-sight (LOS) cases [115]. This is also valid in the interference scenarios for UWB [116]. Many possible combinations of the propagation effects of several environmental characteristics with respect to interference conditions are investigated in detail in reference [117, and therein].

In contrast to nonlayer parameters, there are many parameters that can be populated in the protocol stack. Interference power is one of the fundamental measurement items falling into the physical layer. With the emergence of CR, the term interference power gains additional concepts which have not existed before in previous communication systems such as "interference temperature" and "primary user." Interference temperature is a sort of measure of radio frequency (RF) power that includes power of ambient noise and other interfering signals per unit bandwidth for a receiver antenna. Primary users can be defined as the users who have the higher priority or legacy rights on the usage of a specific part of the spectrum. On the other hand, secondary users are defined as those who (have lower priority) exploit this spectrum in such a way that they do not cause interference to the primary users. Therefore, secondary users need to have the capabilities of CRs, such as sensing the spectrum reliably to check whether it is being used by a primary user and to change the radio parameters to exploit the unused part of the spectrum.[3] Sensing the spectrum for the opportunity is, therefore, one of the most important attributes of CR. Although spectrum sensing is traditionally understood as measuring the spectral content or the interference temperature over the spectrum, when the ultimate CR is considered, it refers to a general term that also involves obtaining the spectrum usage characteristics in multiple dimensions (including time, space, and frequency). When multihop systems are considered, all of these dimensions merge on transmission paths of routing, which is also very important from the network layer standpoint.[4] In such scenarios, some routes might observe more interference than others [118]. Therefore, beside the lower layers, upper layer awareness gains more importance in dealing with interference. Apart from these, determining a comprehensive list of characteristics of signals present in the spectrum (including the modulation, waveform, bandwidth, carrier frequency, duty cycle, application, and so on) is desired for interference awareness in any type of communications system. However, this requires more powerful signal analysis techniques with additional computational complexity. Some of the current challenges in acquiring further information for interference awareness include the following:

1. Difficulty and complexity of wideband sensing, which requires high sampling rate and high-resolution ADC or multiple analog front-end circuitry, high-speed signal processors, and so on. Estimating the noise variance or interference temperature over the transmission of narrowband desired signals is not new. Such noise variance

[3] In Chapter 9, a case study and experimental results for a CR system will be presented, where ZigBee devices can efficiently utilize the available spectrum in the presence of co-channel wireless local area network (WLAN) devices.

[4] Note that single-hop systems do not need to be concerned about such sorts of awareness.

estimation techniques have been popularly used for optimal receiver designs (such as channel estimation and soft information generation), as well as for improved hand-off, power control, and channel allocation techniques. The noise/interference estimation problem is easier for these purposes as the receiver is tuned to receive the signal that is transmitted over the desired bandwidth anyway. Also, the receiver is capable of processing the narrowband baseband signal with reasonably low-complexity and low-power processors. However, CRs are required to process the transmission over a much wider band for sensing any opportunity.

2. Hidden primary user problems (such as the hidden node/terminal problem in carrier sense multiple accessing (CSMA), which can be caused by many reasons including severe multipath fading or shadowing that the secondary user observes in scanning the primary user's transmission. The hidden terminal problem can be avoided by incorporating distributed sensing, where the information sensed between multiple terminals is shared, rather than each terminal making the decision based on its local measurement. One of the examples of distributed sensing is known as spectrum pooling. In this technique [119], cooperative sensing decreases the probability of miss-detections and false alarms considerably. The rental users who are the users that, in case of having spectral opportunities, rent the licensed band temporarily until the licensed user emerges, send their results to a base, which makes a decision and sends the final decision back to the rental users. In this type of scheme, throughout exchanging the sensing information between the base station, the mobile units may create interference to the primary users around. However, this can be overcome by a special signaling scheme which attains a reliable result very fast so that the interference to the primary users can be neglected [119]. Besides, it is again reported in reference [119] that, since this special signaling scheme is not involved with the medium access control (MAC) layer and directly operates on the physical layer, the overhead problem on the network is minimized.
3. Primary users that employ frequency hopping (FH) and spread spectrum signaling, where the power of the primary user signal is distributed over a wider frequency even though the actual information bandwidth is much narrower. Especially, FH-based signaling creates significant problems regarding spectrum sensing. If one knows the hopping pattern, and also perfect synchronization to the signal is achieved, then the problem can be avoided. However, in reality, this is not practical. Approaches based on exploiting the cyclostationarity of the signal have recently been studied to avoid these requirements. The cyclostationary-based techniques exploit the features of the received signal caused by the periodicity in the signal or in its statistics (mean, autocorrelation, and so on).
4. Traffic type is another factor that affects the interference. Statistical characteristics of the traffic type determine the evolution of interference in several dimensions such as time and frequency and help in determining crucial QoS parameters such as link capacity and buffer size and in predicting bandwidth requirements. It is known that different types of traffic exhibit different statistical characteristics. Having the knowledge about the traffic type helps nodes avoid/cancel/minimize interference by different methods such as employing intelligent scheduling. However, it is worth

mentioning that with the increasing services and applications, nodes are expected to be exposed to interference composed of several types of traffic rather than of a single type, including voice, multimedia, and gaming whose statistical characteristics are different from each other. Furthermore, in order to reliably characterize the network traffic, sufficient statistics need to be accumulated in real time.

5. Mobility is crucial for wireless radio communications [120, 121]. From the perspective of interference, mobility introduces further concerns such as mobility behavior [122]. When a MAI environment is of interest, the overall interference becomes a function of mobility behavior of all of the mobile sources within the environment, which can be of individual or of group form. In case victim nodes can extract or are provided with the pattern of the mobility behavior of interfering sources, they can make use of it and improve their performances. Decentralized sensing seems to be a plausible approach for this concern which combines speed and direction information for multiple interference sources.

The interference awareness term actually covers every sort of communications system from short-range to wide area networks (WANs) and to NGWNs, especially those which employ multi-access schemes. Even though fully interference-aware systems which take into account all of the factors listed here may not be implementable in the near future, expanding this list and developing more efficient techniques that are aware of the factors affecting interference are the only solution for the improved communications systems of the future.

8.4 Summary

In this chapter, MAI and NBI mitigation have been studied for UWB systems. Various techniques have been investigated in order to facilitate reliable communications in the presence of interference. In addition, interference awareness has been discussed, which is a very comprehensive term that encompasses many factors. It is clear that better avoidance, cancelation, and mitigation techniques for reliable wireless systems rely on identifying these factors and being aware of them.

References

[1] R. A. Scholtz, "Multiple access with time-hopping impulse modulation," in *Proc. IEEE Military Commun. Conf.*, vol. 2, Bedford, MA, Oct. 1993, pp. 447–450.

[2] M. Z. Win and R. A. Scholtz, "Impulse radio: How it works," *IEEE Commun. Letters*, vol. 2, no. 2, pp. 36–38, Feb. 1998.

[3] ——, "On the energy capture of ultra-wide bandwidth signals in dense multipath environments," *IEEE Commun. Letters*, vol. 2, pp. 245–247, Sep. 1998.

[4] ——, "Ultra-wide bandwidth time-hopping spread-spectrum impulse radio for wireless multiple-access communications," *IEEE Trans. Commun.*, vol. 48, no. 4, pp. 679–691, Apr. 2000.

[5] M. L. Welborn, "System considerations for ultrawideband wireless networks," in *Proc. IEEE Radio and Wireless Conf.*, Boston, MA, Aug. 2001, pp. 5–8.
[6] H. Arslan, Z. N. Chen, and M.-G. D. Benedetto, Eds., *Ultra Wideband Wireless Communications*. Hoboken: Wiley-Interscience, 2006.
[7] S. Gezici, A. F. Molisch, H. Kobayashi, and H. V. Poor, "Low-complexity MMSE combining for linear impulse radio UWB receivers," in *Proc. IEEE Int. Conf. Commun. (ICC)*, Istanbul, Turkey, June 2006, pp. 4706–4711.
[8] C. J. Le-Martret and G. B. Giannakis, "All-digital impulse radio for wireless cellular systems," *IEEE Trans. Commun.*, vol. 50, no. 9, pp. 1440–1450, Sep. 2002.
[9] L. Yang and G. B. Giannakis, "Multi-stage block-spreading for impulse radio multiple access through ISI channels," *IEEE J. Selected Areas in Commun.*, vol. 20, no. 9, pp. 1767–1777, Dec. 2002.
[10] Y.-P. Nakache and A. F. Molisch, "Spectral shape of UWB signals – influence of modulation format, multiple access scheme and pulse shape," in *Proc. IEEE 57th Veh. Technol. Conf. (VTC 2003-Spring)*, vol. 4, Jeju, Korea, Apr. 2003, pp. 2510–2514.
[11] E. Fishler and H. V. Poor, "On the tradeoff between two types of processing gain," *IEEE Trans. Commun.*, vol. 53, no. 10, pp. 1744–1753, Oct. 2005.
[12] S. Gezici, H. Kobayashi, H. V. Poor, and A. F. Molisch, "Performance evaluation of impulse radio UWB systems with pulse-based polarity randomization," *IEEE Trans. Signal Processing*, vol. 53, no. 7, pp. 2537–2549, July 2005.
[13] U. Madhow and M. L. Honig, "On the average near-far resistance for MMSE detection for direct sequence CDMA signals with random spreading," *IEEE Trans. Inf. Theory*, vol. 45, pp. 2039–2045, Sep. 1999.
[14] E. Fishler and H. V. Poor, "Low-complexity multiuser detectors for time-hopping impulse-radio systems," *IEEE Trans. Signal Processing*, vol. 52, no. 9, pp. 2561–2571, Sep. 2004.
[15] S. Verdu, *Multiuser Detection*. 1st ed. Cambridge, UK: Cambridge University Press, 1998.
[16] S. Moshavi, "Multi-user detection for DS-CDMA communications," *IEEE Commun. Mag.*, vol. 34, no. 10, pp. 124–136, Oct. 1996.
[17] Z. Sahinoglu, S. Gezici, and I. Guvenc, *Ultra-Wideband Positioning Systems: Theoretical Limits, Ranging Algorihtm, and Protocols*. New York: Cambridge University Press, 2008.
[18] C. Falsi, D. Dardari, L. Mucchi, and M. Z. Win, "Time of arrival estimation for UWB localizers in realistic environments," *EURASIP J. Applied Sig. Processing*, pp. 1–13, 2006.
[19] D. Dardari and M. Z. Win, "Threshold-based time-of-arrival estimators in UWB dense multipath channels," in *Proc. IEEE Int. Conf. Commun. (ICC)*, vol. 10, Istanbul, Turkey, June 2006, pp. 4723–4728.
[20] I. Guvenc, Z. Sahinoglu, and P. Orlik, "TOA estimation for IR-UWB systems with different transceiver types," *IEEE Trans. Microw. Theory and Techniques (Special Issue on Ultrawideband)*, vol. 54, no. 4, pp. 1876–1886, Apr. 2006.
[21] D. Dardari, C. C. Chong, and M. Z. Win, "Analysis of threshold-based TOA estimator in UWB channels," in *Proc. Euro. Sig. Processing Conf. (EUSIPCO)*, Florence, Italy, Sep. 2006.
[22] D. Dardari, C. C. Chong, and M. Win, "Threshold-based time-of-arrival estimators in UWB dense multipath channels," *IEEE Trans. Commun.*, vol. 56, no. 8, pp. 1366–1378, Aug. 2008.
[23] H. V. Poor, *An Introduction to Signal Detection and Estimation*. New York: Springer-Verlag, 1994.

[24] Y. C. Yoon and R. Kohno, "Optimum multi-user detection in ultrawideband (UWB) multiple-access communication systems," in *Proc. IEEE Int. Conf. Commun. (ICC)*, New York City, NY, Apr. 2002, pp. 812–816.

[25] I. Guvenc and H. Arslan, "A review on multiple access interference cancellation and avoidance for IR-UWB," *Elsevier Signal Processing J.*, vol. 87, no. 4, pp. 623–653, Apr. 2007.

[26] S. Gezici, H. Kobayashi, and H. V. Poor, "A comparative study of pulse combining schemes for impulse radio UWB systems," in *Proc. IEEE Sarnoff Symp.*, Princeton, NJ, Apr. 2004, pp. 7–10.

[27] W. M. Lovelace and J. K. Townsend, "Chip discrimination for large near-far power ratios in UWB networks," in *Proc. IEEE Military Commun. Conf. (MILCOM)*, vol. 2, Boston, MA, Oct. 2003, pp. 868–873.

[28] S. Gezici, H. Kobayashi, H. V. Poor, and A. F. Molisch, "Performance evaluation of impulse radio UWB systems with pulse-based polarity randomization," *IEEE Trans. Signal Processing*, vol. 53, no. 7, pp. 2537–2549, July 2005.

[29] S. Gezici, M. Chiang, H. V. Poor, and H. Kobayashi, "Optimal and suboptimal finger selection algorithms for MMSE Rake receivers in impulse radio ultrawideband systems," *EURASIP J. Wireless Commun. and Networking*, vol. 2006, no. 7, 2006, article ID 84249.

[30] S. Gezici, H. V. Poor, H. Kobayashi, and A. F. Molisch, "Optimal and suboptimal linear receivers for impulse radio UWB systems," in *Proc. IEEE Int. Conf. on Ultra-Wideband (ICUWB)*, Waltham, MA, Sep. 2006, pp. 161–166.

[31] S. Gezici, H. Kobayashi, H. V. Poor, and A. F. Molisch, "Optimal and suboptimal linear receivers for time-hopping impulse radio systems," in *Proc. IEEE Conf. on Ultra Wideband Systems and Technologies (UWBST)*, Kyoto, Japan, May 2004, pp. 11–15.

[32] C. J. Le-Martret and G. B. Giannakis, "All-digital PAM impulse radio for multiple-access through frequency-selective multipath," in *Proc. IEEE Global Telecommun. Conf. (GLOBECOM)*, vol. 1, San Francisco, CA, Nov. 2000, pp. 77–81.

[33] H. V. Poor, "Iterative multiuser detection," *IEEE Signal Processing Mag.*, vol. 21, no. 1, pp. 81–88, Jan. 2004.

[34] A. R. Forouzan, M. Nasiri-Kenari, and J. A. Salehi, "Performance analysis of time-hopping spread-spectrum multiple-access systems: Uncoded and coded schemes," *IEEE Trans. on Wireless Commun.*, vol. 1, no. 4, pp. 671–681, Oct. 2002.

[35] A. Bayesteh and M. Nasiri-Kenari, "Iterative interference cancellation and decoding for a coded UWB-TH-CDMA system in AWGN channel," in *Proc. IEEE Int. Symp. on Spread Spectrum Techniques and Applications*, vol. 1, Prague, Czech Republic, Sep. 2002, pp. 263–267.

[36] ——, "Iterative interference cancellation and decoding for a coded UWB-TH-CDMA system in multipath channels using MMSE filters," in *Proc. IEEE Int. Symp. on Personal, Indoor and Mobile Radio Communications (PIMRC)*, vol. 2, Sep. 2003, pp. 1555–1559.

[37] K. Takizawa and R. Kohno, "Combined iterative demapping and decoding for coded UWB-IR systems," in *Proc. IEEE Conf. on Ultra Wideband Syst. and Technol. (UWBST)*, Reston, VA, Nov. 2003, pp. 423–427.

[38] N. Yamamoto and T. Ohtsuki, "Adaptive internally turbo-coded ultra wideband-impulse radio (AITC-UWB-IR) system," in *Proc. IEEE Int. Conf. on Commun. (ICC)*, vol. 5, Anchorage, AK, May 2003, pp. 3535–3539.

[39] E. Fishler, S. Gezici, and H. V. Poor, "Iterative ("turbo") multiuser detectors for impulse radio systems," *IEEE Trans. on Wireless Commun.*, vol. 7, no. 8, pp. 2964–2974, Aug. 2008.

[40] J. Foerster, "Channel modeling sub-committee report final, IEEE802.15-02/490," 2002. [Online]. Available: http://ieee802.org/15

[41] D. Cassioli, M. Z. Win, F. Vatalaro, and A. F. Molisch, "Performance of low-complexity RAKE reception in a realistic UWB channel," in *Proc. IEEE Int. Conf. Commun. (ICC)*, vol. 2, New York City, NY, Apr. 2002, pp. 763–767.

[42] Z. Xu, J. Tang, and P. Liu, "Frequency-domain estimation of multiple access ultrawideband signals," in *Proc. IEEE Workshop on Statistical Signal Processing*, Louis, MO, Sep. 2003, pp. 74–77.

[43] S. Morosi and T. Bianchi, "Frequency domain multiuser detectors for ultrawideband short-range communications," in *Proc. IEEE Conf. on Acoust., Speech, Sig. Processing (ICASSP)*, vol. 3, Quebec, Canada, Mar. 2004, pp. 637–640.

[44] Y. Tang, B. Vucetic, and Y. Li, "An FFT-based multiuser detection for asynchronous block-spreading CDMA ultrawideband communication systems," in *Proc. IEEE Int. Conf. on Commun. (ICC)*, vol. 5, Seoul, Korea, 2005, pp. 2872–2876.

[45] A. M. Tonello and R. Rinaldo, "Frequency domain multiuser detection for impulse radio systems," in *Proc. IEEE Veh. Technol. Conf.*, vol. 2, Stockholm, Sweden, May 2005, pp. 1381–1385.

[46] H. Hotelling, "Analysis of a complex of statistical variables into principal component," *J. Educ. Psychol.*, vol. 24, pp. 417–441, 498–520, 1933.

[47] C. Eckart and G. Young, "The approximation of one matrix by another of lower rank," *Psychometrica*, vol. 1, pp. 211–218, 1936.

[48] P. Liu, Z. Xu, and J. Tang, "Subspace multiuser receivers for UWB communication systems," in *Proc. IEEE Conf. on Ultra Wideband Systems and Technologies (UWBST)*, Reston, VA, Nov. 2003, pp. 16–19.

[49] J. S. Goldstein, I. S. Reed, and L. L. Scharf, "A multistage representation of the Wiener filter based on orthogonal projections," *IEEE Trans. Inf. Theory*, vol. 44, no. 7, pp. 2943–2959, Nov. 1998.

[50] W. Sau-Hsuan, U. Mitra, and C.-C. J. Kuo, "Multistage MMSE receivers for ultra-wide bandwidth impulse radio communications," in *Proc. IEEE Conf. on Ultra Wideband Systems and Technologies (UWBST)*, Kyoto, Japan, May 2004, pp. 16–20.

[51] M. L. Honig and W. Xiao, "Performance of reduced-rank linear interference suppression," *IEEE Trans. Inf. Theory*, vol. 47, no. 5, pp. 1928–1946, July 2001.

[52] A. Muqaibel, B. Woerner, and S. Riad, "Application of multiuser detection techniques to impulse radio time hopping multiple access systems," in *Proc. IEEE Conf. on Ultra Wideband Syst. Technol. (UWBST)*, Baltimore, MD, May 2002, pp. 169–173.

[53] N. Boubaker and K. B. Letaief, "Combined multiuser successive interference cancellation and partial RAKE reception for ultrawideband wireless communications," in *Proc. IEEE Veh. Technol. Conf.*, vol. 2, Los Angeles, CA, Sep. 2004, pp. 1209–1212.

[54] D. H. S. Han, C.C. Woo, "UWB interference cancellation receiver in dense multipath fading channel," in *Proc. IEEE Veh. Technol. Conf.*, vol. 2, Milan, Italy, May 2004, pp. 1233–1236.

[55] Z. Xu, P. Liu, and J. Tang, "Blind multiuser detection for impulse radio UWB systems," in *Proc. IEEE Topical Conf. on Wireless Commun. Technol.*, Honolulu, HI, Oct. 2003, pp. 453–454.

[56] P. Liu, Z. Xu, and J. Tang, "Minimum variance multiuser detection for impulse radio UWB systems," in *Proc. IEEE Conf. on Ultra Wideband Syst. Technol. (UWBST)*, Reston, VA, Nov. 2003, pp. 111–115.

[57] P. Liu and Z. Xu, "Performance of POR multiuser detection for UWB communications," in *Proc. IEEE Conf. on Acoust., Speech, Sig. Processing (ICASSP)*, Philadelphia, PA, Mar. 2005.

[58] M. S. Iacobucci and M. G. D. Benedetto, "Multiple access design for impulse radio communication systems," in *Proc. IEEE Int. Conf. Commun. (ICC)*, vol. 2, New York City, NY, Apr. 2002, pp. 817–820.

[59] T. Erseghe, "Time-hopping patterns derived from permutation sequences for ultrawideband impulse-radio applications," in *Proc. WSEAS Int. Conf. on Commun.*, vol. 1, Crete, July 2002, pp. 109–115.

[60] I. Guvenc and H. Arslan, "Design and performance analysis of TH sequences for UWB-IR systems," in *Proc. IEEE Wireless Commun. and Networking Conf. (WCNC)*, vol. 2, Atlanta, GA, Mar. 2004, pp. 914–919.

[61] ——, "TH sequence construction for centralised UWB-IR systems in dispersive channels," *IEE Electron. Lett.*, vol. 40, no. 8, pp. 491–492, Apr. 2004.

[62] I. Guvenc, H. Arslan, S. Gezici, and H. Kobayashi, "Adaptation of two types of processing gains for UWB impulse radio wireless sensor networks," *IET Commun.*, vol. 1, no. 6, pp. 1280–1288, Dec. 2007.

[63] O. Moreno and S. V. Maric, "A new family of frequency-hop codes," *IEEE Trans. Commun.*, vol. 48, no. 8, pp. 1241–1244, Aug. 2000.

[64] G. M. Maggio, N. Rulkov, and L. Reggiani, "Pseudo-chaotic time hopping for UWB impulse radio," *IEEE Trans. Circuits and Syst. I: Fundamental Theory and Applications*, vol. 48, no. 12, pp. 1424–1435, Dec. 2001.

[65] G. M. Maggio, D. Laney, F. Lehmann, and L. Larson, "A multi-access scheme for UWB radio using pseudo-chaotic time hopping," in *Proc. IEEE Conf. on Ultra Wideband Syst. Technol. (UWBST)*, Baltimore, MD, May 2002, pp. 225–229.

[66] D. C. Laney, G. M. Maggio, F. Lehmann, and L. Larson, "Multiple access for UWB impulse radio with pseudochaotic time hopping," *IEEE J. on Selected Areas in Commun.*, vol. 20, no. 9, pp. 1692–1700, Dec. 2002.

[67] L. Yang and G. B. Giannakis, "Ultra-wideband communications: An idea whose time has come," *IEEE Sig. Processing Mag.*, vol. 21, no. 6, pp. 26–54, Nov. 2004.

[68] J. Foerster, "Ultra-wideband technology enabling low-power, high-rate connectivity (invited paper)," in *Proc. IEEE Workshop Wireless Commun. Networking*, Pasadena, CA, Sep. 2002.

[69] J. R. Foerster, "The performance of a direct-sequence spread ultrawideband system in the presence of multipath, narrowband interference, and multiuser interference," in *Proc. IEEE Veh. Technol. Conf.*, vol. 4, Birmingham, AL, May 2002, pp. 1931–1935.

[70] K. Shi, Y. Zhou, B. Kelleci, T. Fischer, E. Serpedin, and A. Karsilayan, "Impacts of narrowband interference on OFDM-UWB receivers: Analysis and mitigation," *IEEE Trans. Signal Proc.*, vol. 55, no. 3, p. 1118, 2007.

[71] C. da Silva and L. Milstein, "The effects of narrowband interference on UWB communication systems with imperfect channel estimation," *IEEE J. Select. Areas Commun.*, vol. 24, no. 4, pp. 717–723, 2006.

[72] Y. Alemseged and K. Witrisal, "Modeling and mitigation of narrowband interference for transmitted-reference UWB systems," *IEEE J. Select. Topics Signal Proc.*, vol. 1, no. 3, p. 456, 2007.

[73] L. Zhao and A. Haimovich, "Performance of ultrawideband communications in the presence of interference," *IEEE J. Select. Areas Commun.*, vol. 20, pp. 1684–1691, Dec. 2002.

[74] G. Durisi and S. Benedetto, "Performance evaluation of TH-PPM UWB systems in the presence of multiuser interference," *IEEE Commun. Lett.*, vol. 7, no. 5, pp. 224–226, May 2003.

[75] J. Choi and N. Cho, "Narrow-band interference suppression in direct sequence spread spectrum systems using a lattice IIR notch filter," in *Proc. IEEE Int. Conf. Acoustics, Speech, Signal Processing (ICASSP)*, vol. 3, Munich, Germany, April 1997, pp. 1881–1884.

[76] L. Rusch and H. Poor, "Multiuser detection techniques for narrowband interference suppression in spread spectrum communications," *IEEE Trans. Commun.*, vol. 42, pp. 1727–1737, Apr. 1995.

[77] J. Proakis, "Interference suppression in spread spectrum systems," in *Proc. IEEE Int. Symp. on Spread Spectrum Techniques and Applications*, vol. 1, Sep. 1996, pp. 259–266.

[78] L. Milstein, "Interference rejection techniques in spread spectrum communications," in *Proc. IEEE*, vol. 76, June 1988, pp. 657–671.

[79] C. Carlemalm, H. V. Poor, and A. Logothetis, "Suppression of multiple narrowband interferers in a spread-spectrum communication system," *IEEE J. Select. Areas Commun.*, vol. 18, no. 8, pp. 1365–1374, Aug. 2000.

[80] P. Azmi and M. Nasiri-Kenari, "Narrow-band interference suppression in CDMA spread-spectrum communication systems based on sub-optimum unitary transforms," *IEICE Trans. Commun.*, vol. E85-B, No.1, pp. 239–246, Jan. 2002.

[81] T. J. Lim and L. K. Rasmussen, "Adaptive cancellation of narrowband signals in overlaid CDMA systems," in *Proc. IEEE Int. Workshop Intel. Signal Processing and Commun. Syst.*, Singapore, Nov. 1996, pp. 1648–1652.

[82] H. Fathallah and L. Rusch, "Enhanced blind adaptive narrowband interference suppression in DSSS," in *Proc. IEEE Global Telecommun. Conf. (GLOBECOM)*, vol. 1, London, UK, Nov. 1996, pp. 545–549.

[83] W.-S. Hou, L.-M. Chen, and B.-S. Chen, "Adaptive narrowband interference rejection in DS-CDMA systems: A scheme of parallel interference cancellers," *IEEE J. Select. Areas Commun.*, vol. 20, pp. 1103–1114, June 2001.

[84] P.-R. Chang, "Narrowband interference suppression in spread spectrum CDMA communications using pipelined recurrent neural networks," in *Proc. IEEE Int. Conf. Universal Personal Commun. (ICUPC)*, vol. 2, Oct. 1998, pp. 1299–1303.

[85] H. V. Poor and X. Wang, "Code-aided interference suppression in DS/CDMA spread spectrum communications," *IEEE Trans. Commun.*, vol. 45, no. 9, pp. 1101–1111, Sept. 1997.

[86] S. Buzzi, M. Lops, and A. Tulino, "Time-varying MMSE interference suppression in asynchronous DS/CDMA systems over multipath fading channels," in *Proc. IEEE Int. Symp. on Personal, Indoor and Mobile Radio Commun.*, Sep. 1998, pp. 518–522.

[87] M. Medley, "Narrow-band interference excision in spread spectrum systems using lapped transforms," *IEEE Trans. Commun.*, vol. 45, pp. 1444–1455, Nov. 1997.

[88] A. Akansu, M. Tazebay, M. Medley, and P. Das, "Wavelet and subband transforms: Fundamentals and communication applications," *IEEE Commun. Mag.*, vol. 35, pp. 104–115, Dec. 1997.

[89] B. Krongold, M. Kramer, K. Ramchandran, and D. Jones, "Spread spectrum interference suppression using adaptive time-frequency tilings," in *Proc. IEEE Int. Conf. Acoustics, Speech, Signal Processing (ICASSP)*, vol. 3, Munich, Germany, April 1997, pp. 1881–1884.

[90] Y. Zhang and J. Dill, "An anti-jamming algorithm using wavelet packet modulated spread spectrum," in *Proc. IEEE Military Commun. Conf.*, vol. 2, Nov 1999, pp. 846–850.
[91] T. Kasparis, "Frequency independent sinusoidal suppression using median filters," in *Proc. IEEE Int. Conf. Acoustics, Speech, Signal Processing (ICASSP)*, vol. 3, Toronto, Canada, April 1991, pp. 612–615.
[92] D. Zhang, P. Fan, and Z. Cao, "Interference cancellation for OFDM systems in presence of overlapped narrow band transmission system," *IEEE Consum. Electron.*, 2004.
[93] R. Lowdermilk and F. Harris, "Interference mitigation in orthogonal frequency division multiplexing (OFDM)," in *Proc. IEEE Int. Conf. Universal Personal Commun. (ICUPC)*, vol. 2, Cambridge, MA, Sep. 1996, pp. 623–627.
[94] R. Nilsson, F. Sjoberg, and J. LeBlanc, "A rank-reduced lmmse canceller for narrowband interference suppression in OFDM-based systems," *IEEE Trans. Commun.*, vol. 51, no. 12, pp. 2126–2140, Dec. 2003.
[95] M. Ghosh and V. Gadam, "Bluetooth interference cancellation for 802.11g WLAN receivers," in *Proc. IEEE Int. Conf. Commun. (ICC)*, vol. 2, Anchorage, AK, May 2003, pp. 1169–1173.
[96] M. Z. Win and R. A. Scholtz, "Impulse radio: How it works," *IEEE Commun. Lett.*, vol. 2, no. 2, pp. 36–38, Feb. 1998.
[97] X. Chu and R. Murch, "The effect of NBI on UWB time-hopping systems," *IEEE Trans. on Wireless Commun.*, vol. 3, no. 5, pp. 1431–1436, Sep. 2004.
[98] A. Taha and K. Chugg, "A theoretical study on the effects of interference on UWB multiple access impulse radio," in *Proc. IEEE Asilomar Conf. on Signals, Syst., Comput.*, vol. 1, Pacific Grove, CA, Nov 2002, pp. 728–732.
[99] I. Guvenc and H. Arslan, "Performance evaluation of UWB systems in the presence of timing jitter," in *Proc. IEEE Ultra Wideband Syst. Technol. Conf.*, Reston, VA, Nov 2003, pp. 136–141.
[100] L. Piazzo and J. Romme, "Spectrum control by means of the TH code in UWB systems," in *Veh. Technol. Conf.*, vol. 3, Apr. 2003, pp. 1649–1653.
[101] ——, "On the power spectral density of time-hopping impulse radio," in *IEEE Conf. Ultrawideband Syst. Technol. (UWBST)*, May 2002, pp. 241–244.
[102] H. Schantz, G. Wolenec, and E. Myszka, "Frequency notched UWB antennas," in *IEEE Conf. Ultrawideband Syst. Technol. (UWBST)*, vol. 3, Nov. 2003, pp. 214–218.
[103] I. Bergel, E. Fishler, and H. Messer, "Narrowband interference suppression in impulse radio systems," in *IEEE Conf. on UWB Syst. Technol.*, Baltimore, MD, May 2002, pp. 303–307.
[104] S. Verdu, *Multiuser Detection*. 1st ed. Cambridge, UK: Cambridge University Press, 1998.
[105] R. Klein, M. Temple, R. Raines, and R. Claypoole, "Interference avoidance communications using wavelet domain transformation techniques," *Electron. Lett.*, vol. 37, no. 15, pp. 987–989, July 2001.
[106] M. Medley, G. Saulnier, and P. Das, "Radiometric detection of direct-sequence spread spectrum signals with interference excision using the wavelet transform," in *IEEE Int. Conf. on Commun. (ICC 94)*, vol. 3, May 1994, pp. 1648–1652.
[107] J. Patti, S. Roberts, and M. Amin, "Adaptive and block excisions in spread spectrum communication systems using the wavelet transform," in *Asilomar Conf. on Signals, Syst., Computers*, vol. 1, Nov. 1994, pp. 293–297.
[108] X. Wang and H. V. Poor, *Wireless Communication Systems: Advanced Techniques for Signal Reception*. 1st ed., Upper Saddle River, NJ: Prentice Hall, 2004.

[109] C. W. Rhodes, "Reduction of NTSC co–channel interference by referencing carrier frequencies to the LORAN–C signal," *IEEE Trans. on Broadcasting*, vol. 41, no. 2, pp. 37–43, June 1995.

[110] B. L. Cragin, "Prediction of seasonal trends in cellular dropped call probability," in *Proc. IEEE Int. Conf. on Electro/Inf. Technol.*, East Lansing, Michigan, USA, May 7–10, 2006, pp. 613–618.

[111] Y. Pinhasi and A. Yahalom, "Spectral characteristics of gaseous media and their effects on propagation of ultrawideband radiation in the millimeter wavelengths," *J. Non-Crystalline Solids*, vol. 351, no. 33–36, pp. 2925–2928, 2005.

[112] A. R. S. Bahai and H. Aghvami, "Network planning and optimization in the third generation wireless networks," in *Proc. First Int. Conf. on 3G Mobile Commun. Technologies*, London, UK, Mar. 27–29, 2000, pp. 441–445.

[113] V. M. Jovanovic and J. Gazzola, "Capacity of present narrowband cellular systems: Interference-limited or blocking-limited?" *IEEE Personal Commun. [see also IEEE Wireless Commun.]*, vol. 4, no. 6, pp. 42–51, Dec. 1997.

[114] S. Farahvash and M. Kavehrad, "Co-channel interference assessment for line-of-sight and nearly line-of-sight millimeter-waves cellular LMDS architecture," *Int. J. Wireless Inf. Networks*, vol. 7, no. 4, pp. 197–210, 2000.

[115] M. Yang, D. Kaffes, D. Mavrakis, and S. Stavrou, "The impact of environment variation on co-channel interference in WLAN," in *Proc. Twelfth Int. Conf. on Antennas and Propagation (ICAP 2003)*, vol. 1. University of Exeter, UK: IEE, Mar. 31– Apr. 3, 2003, pp. 71–75.

[116] Q. Li and L. A. Rusch, "Multiuser detection for DS–CDMA UWB in the home environment," *IEEE J. on Selected Areas in Commun.*, vol. 20, no. 9, pp. 1701–1711, Dec. 2002.

[117] G. L. Stüber, *Principles of Mobile Communications*. Kluwer Academic Publishers, 1996, 4th printing.

[118] R. Menon, A. B. MacKenzie, R. M. Buehrer, and J. H. Reed, "A game–theoretic framework for interference avoidance in ad hoc networks," in *Proc. IEEE Global Telecommun. Conf. (GLOBECOM '06)*, vol. 1, San Francisco, CA, Nov. 27– Dec. 1, 2006, pp. 1–6.

[119] T. Weiss and F. K. Jondral, "Spectrum pooling: An innovative strategy for the enhancement of spectrum efficiency," *IEEE Commun. Mag.*, vol. 42, no. 3, pp. S8–14, Mar. 2004.

[120] Y.-D. Yao and A. U. H. Sheikh, "Investigations into co-channel interference in microcellular mobile radio systems," *IEEE Trans. on Veh. Technol.*, vol. 41, no. 2, pp. 114–123, May 1992.

[121] B. C. Jones and D. J. Skellern, "An integrated propagation–mobility interference model for microcell network coverage prediction," *Wireless Personal Commun.*, vol. 5, pp. 223–258, 1997.

[122] S. Yarkan, A. Maaref, K. H. Teo, and H. Arslan, "Impact of mobility on the behavior of interference in cellular wireless networks," in *Proc. IEEE Global Commun. Conf. (GLOBECOM 2008)*, New Orleans, LA, Nov. 30–Dec. 4, 2008.